Registering (aligning) multiple topographic datasets and topographic change detection

The **Iterative Closest Point** algorithm: a method for registering (aligning) two sets of points

Fig. 4. Iterative point-based registration of phantom face range data

point cloud #1

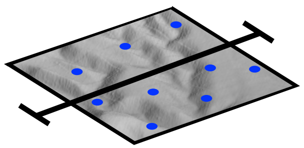

point cloud #2

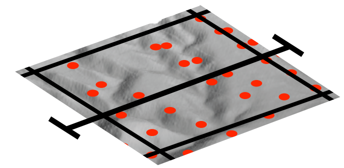

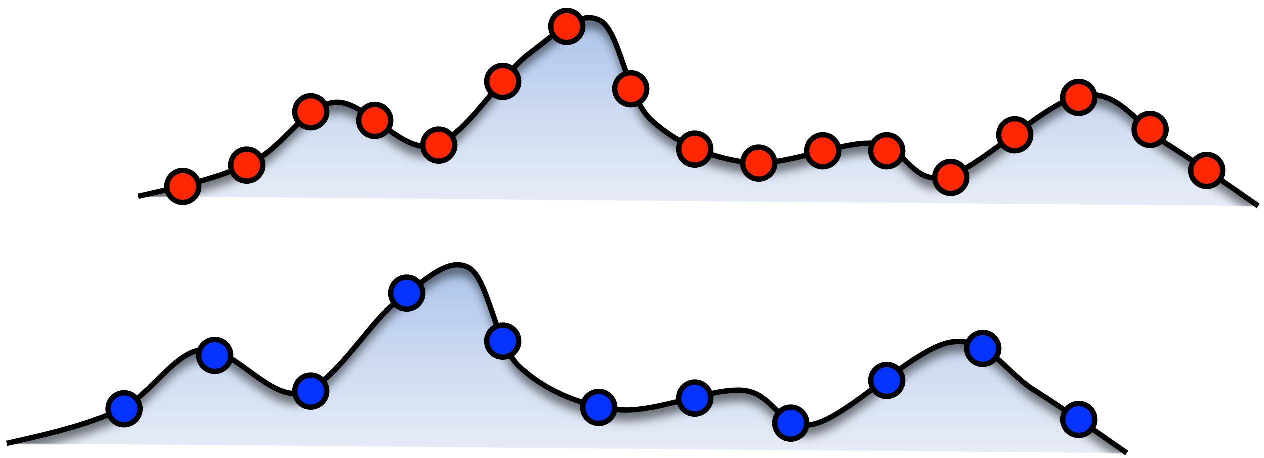

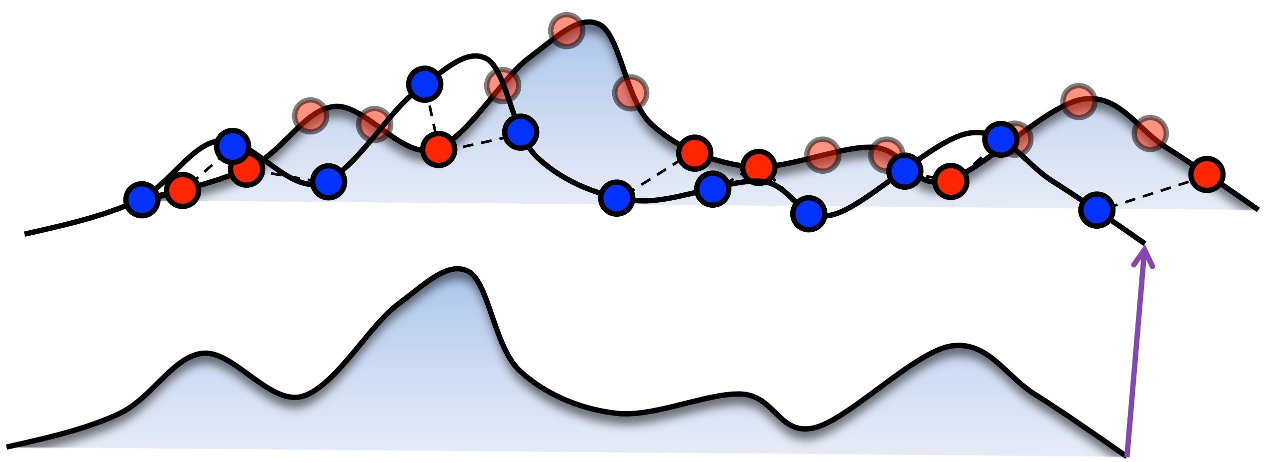

Iterate

Find closest points

Transform point cloud

$$\phi = \begin{pmatrix} 1 & -\gamma & \beta & t_x \\ \gamma & 1 & -\alpha & t_y \\ -\beta & \alpha & 1 & t_z \\ 0 & 0 & 0 & 1 \end{pmatrix}$$

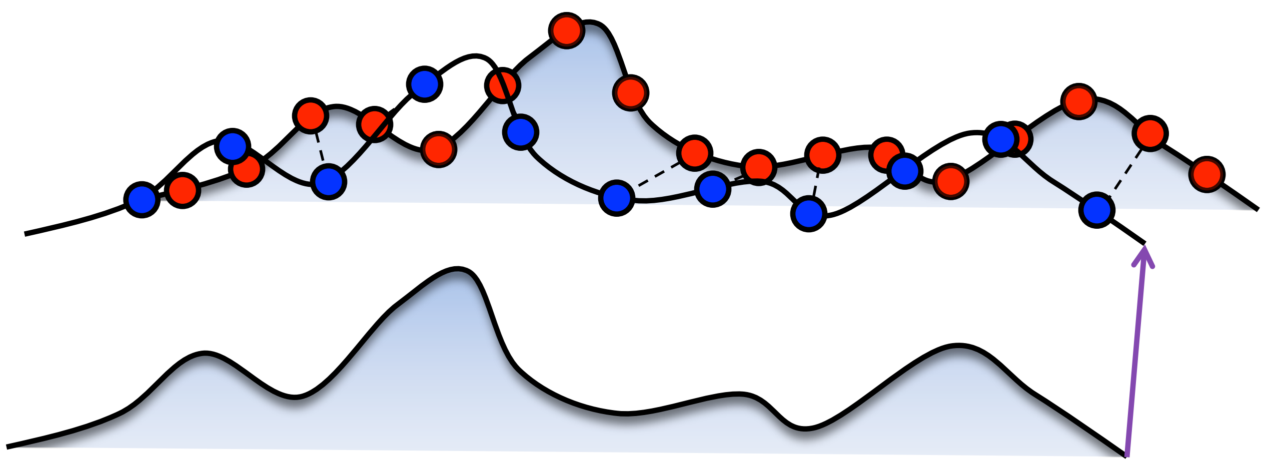

Find closest points

Transform point cloud

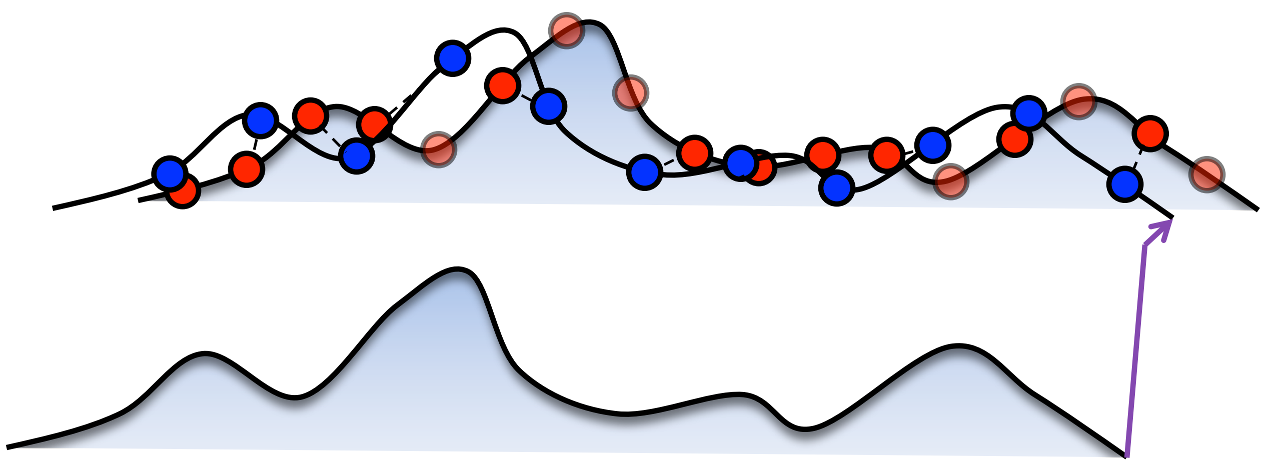

Find closest points

Transform point cloud

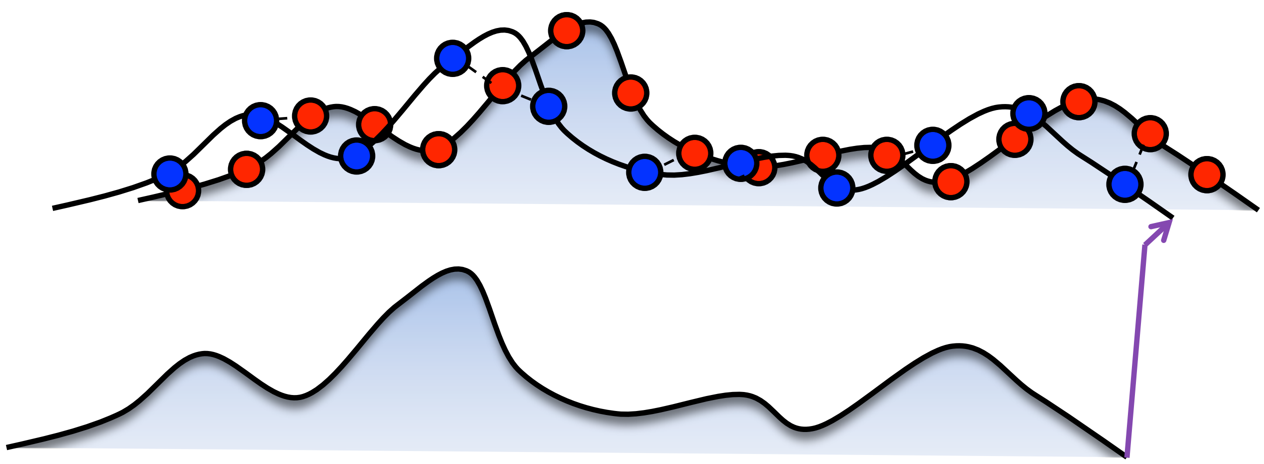

Find closest points

Transform point cloud

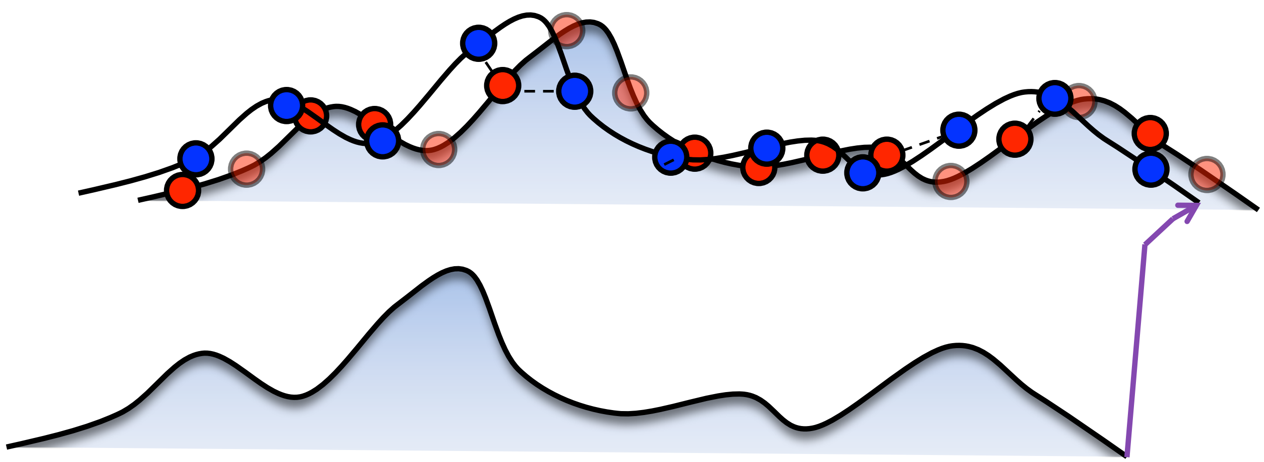

Find closest points

Transform point cloud

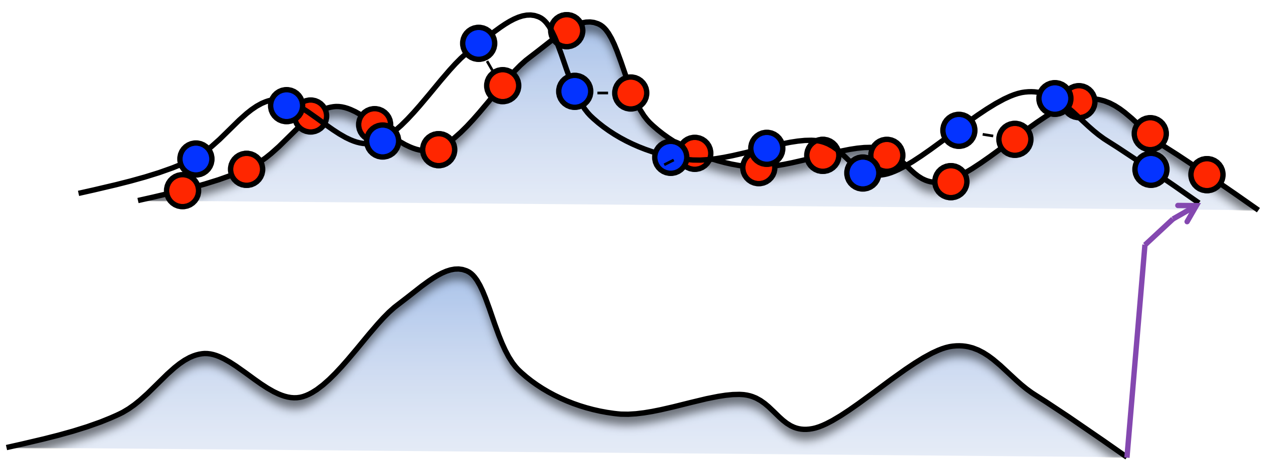

Find closest points

Transform point cloud

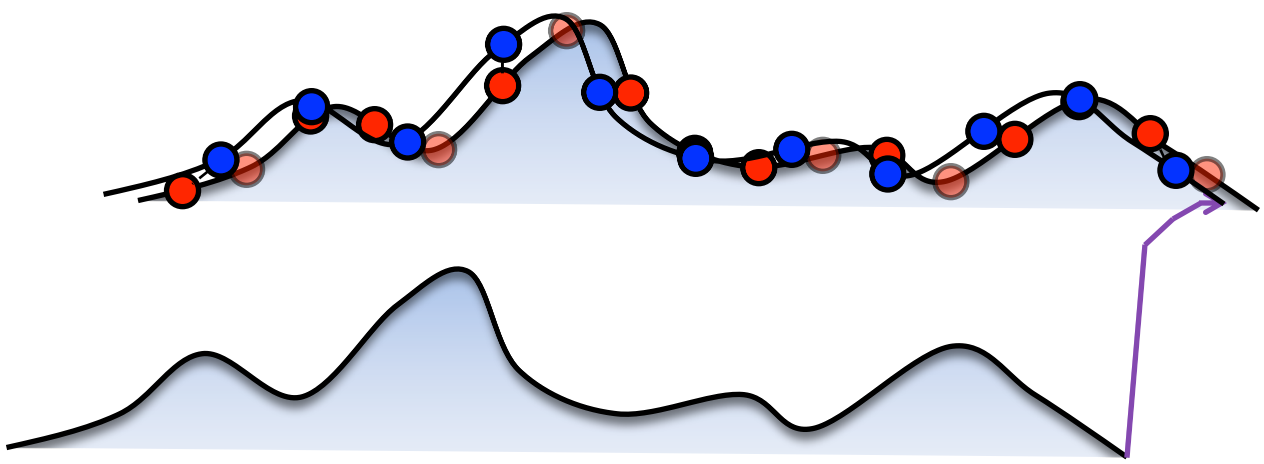

Find closest points

Transform point cloud

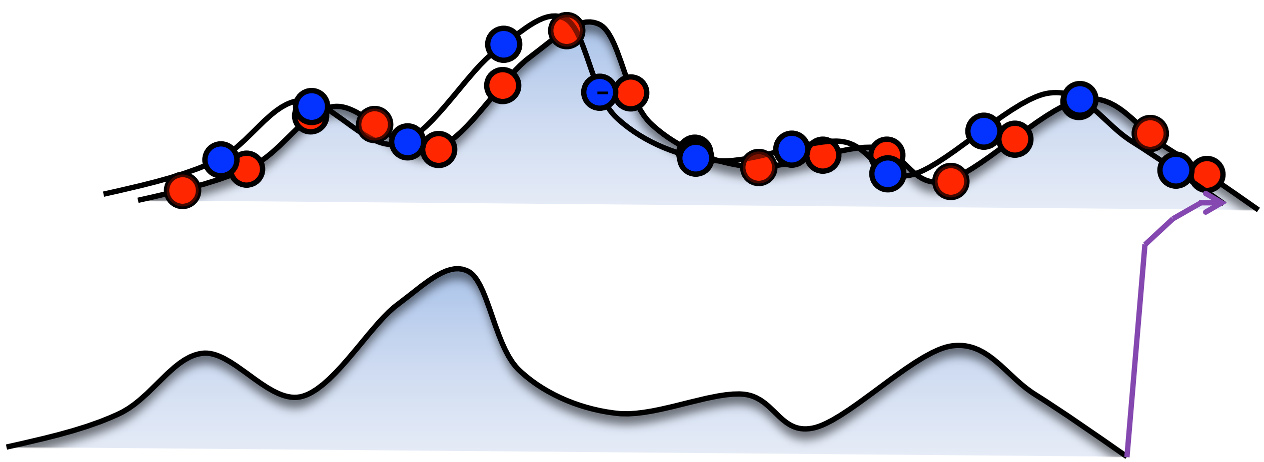

Find closest points

Transform point cloud

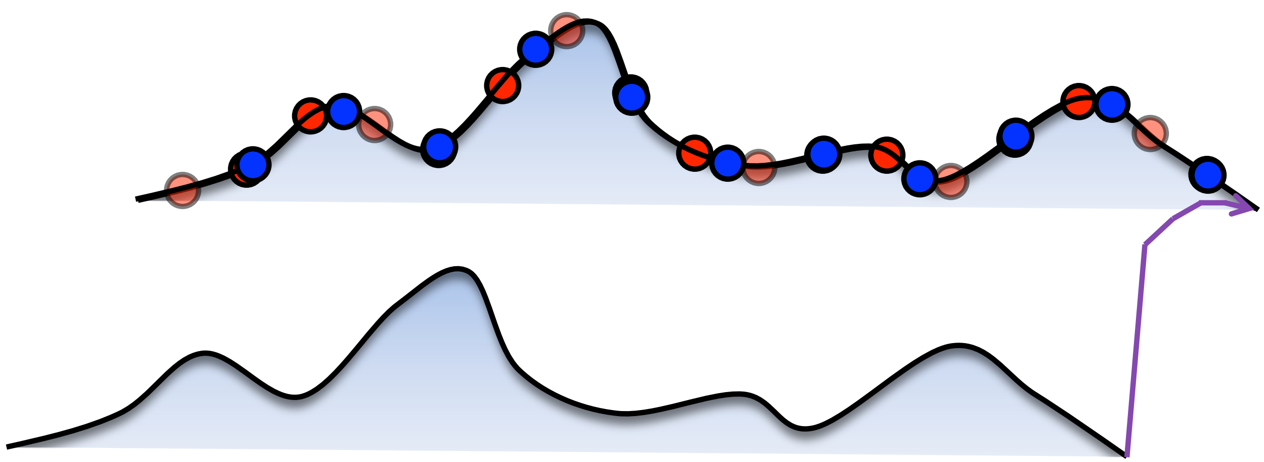

Find closest points

Transform point cloud

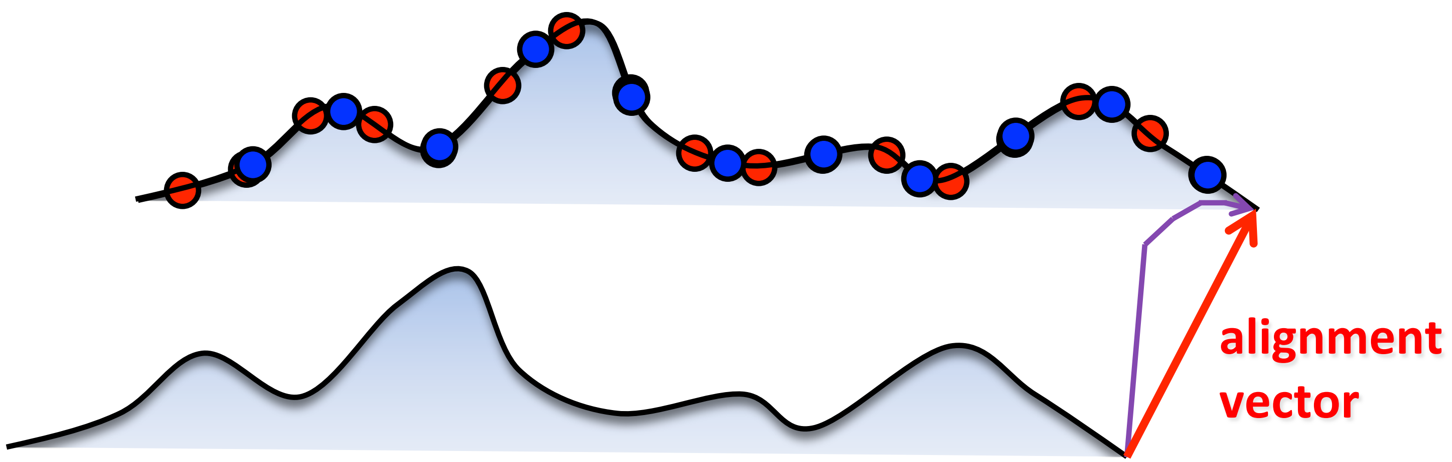

Find closest points

Transform point cloud

Pre-earthquake LiDAR survey

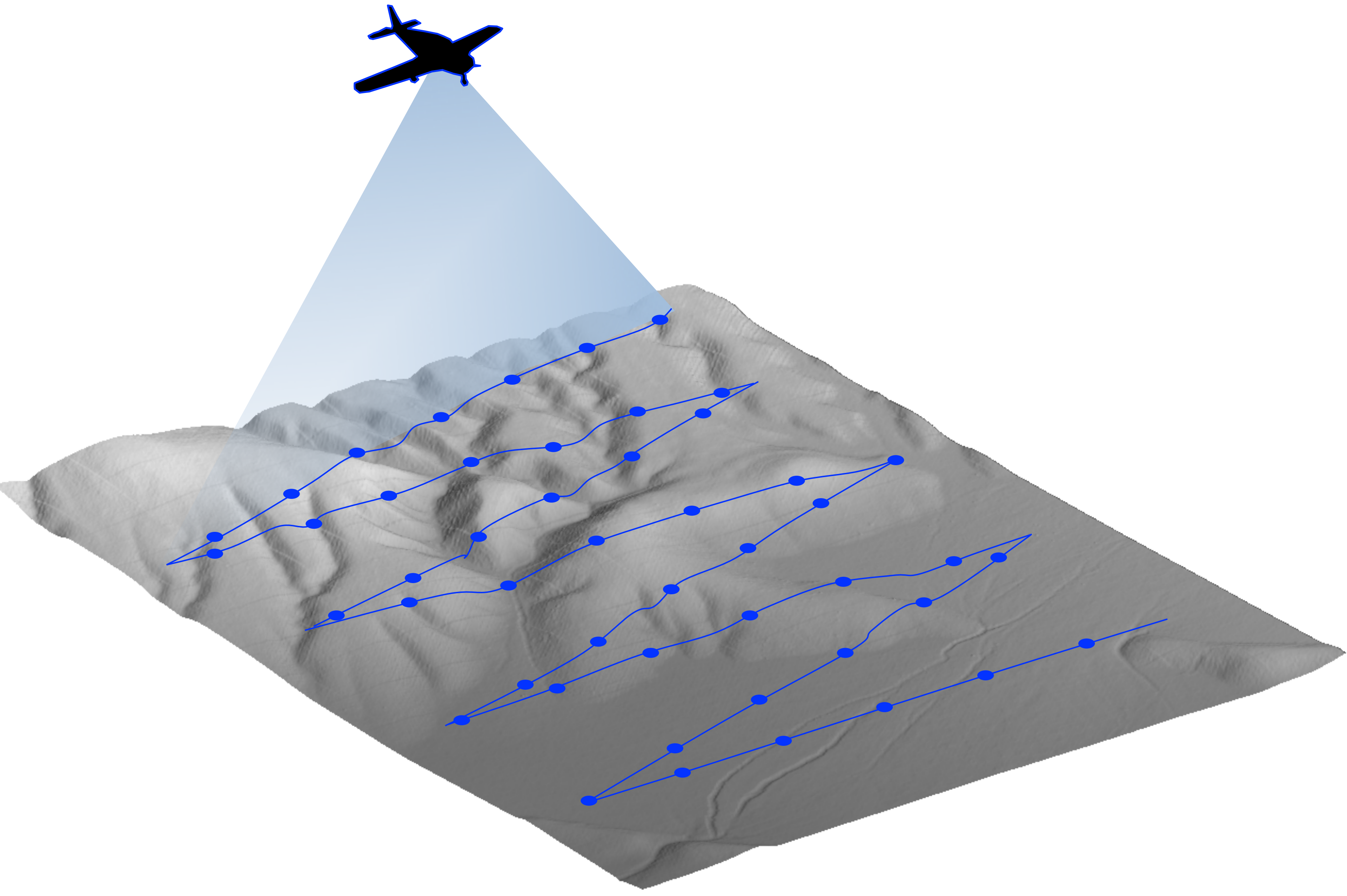

Pre-earthquake point cloud

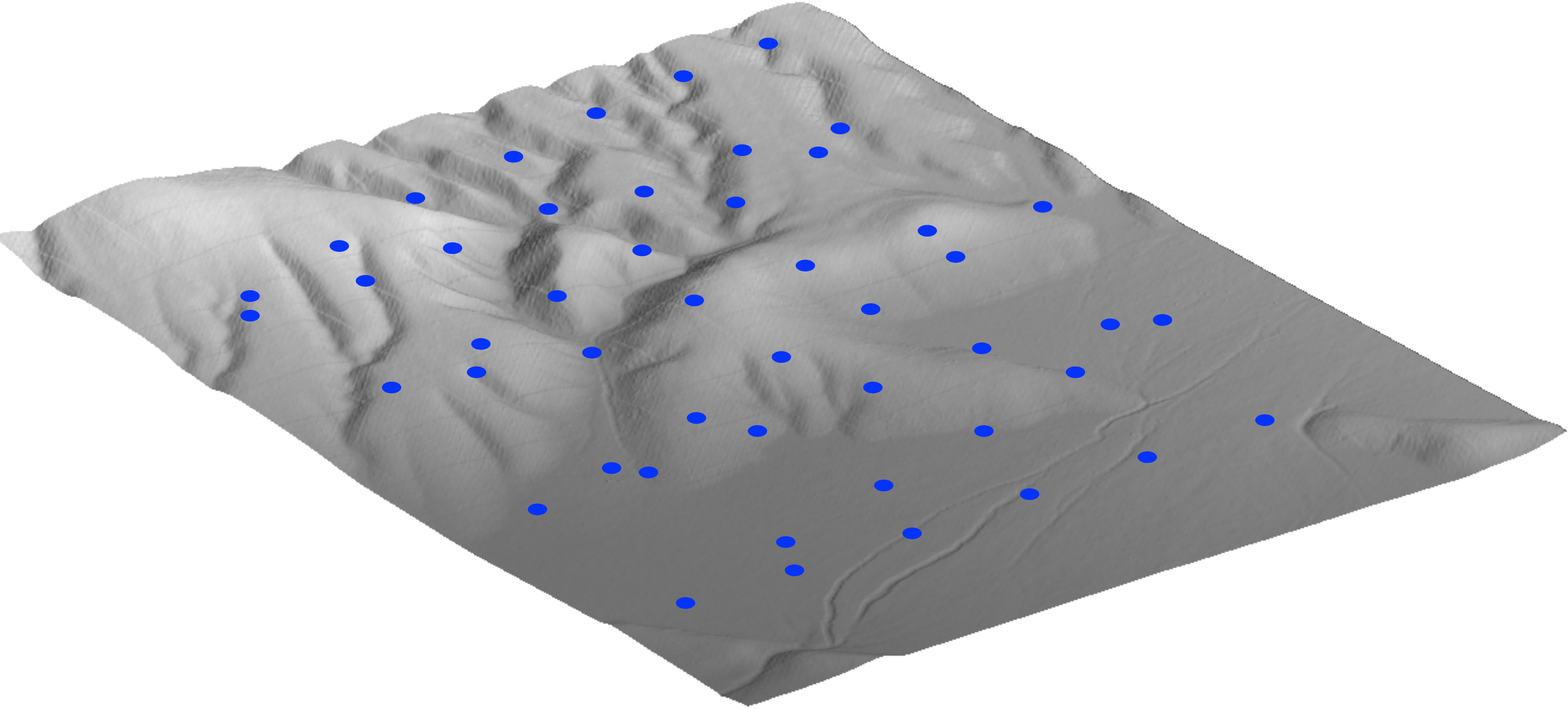

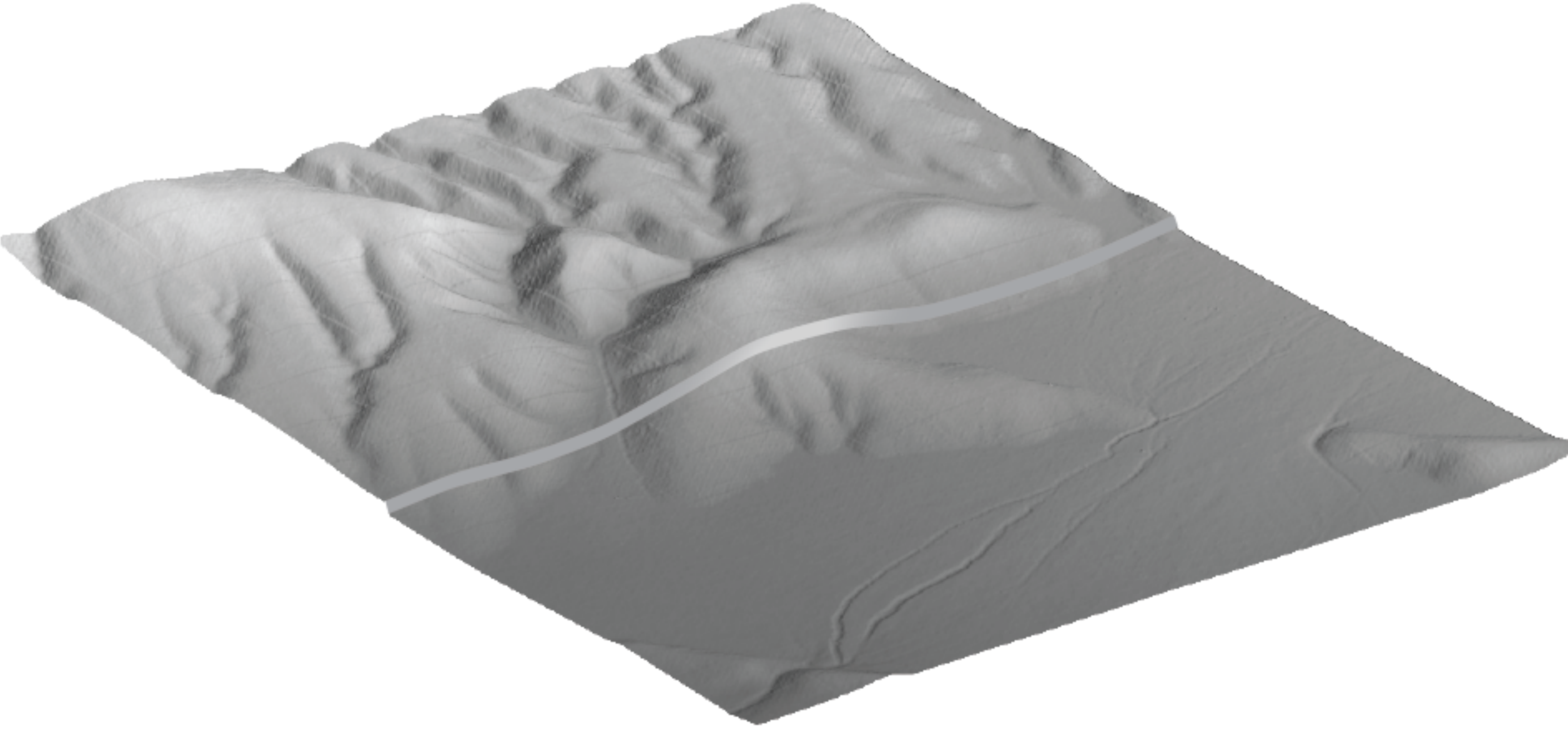

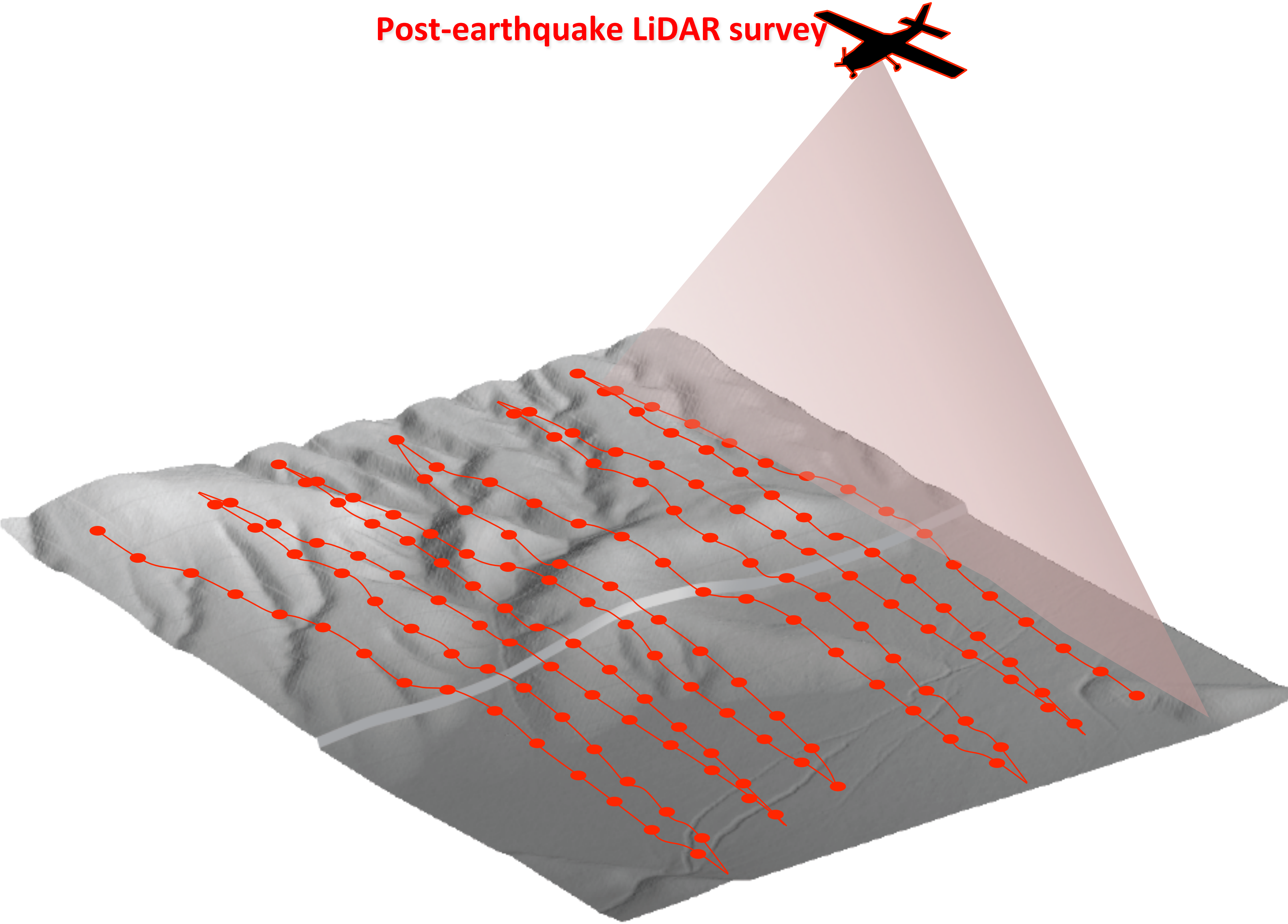
Post-earthquake LiDAR survey

Post-earthquake point cloud

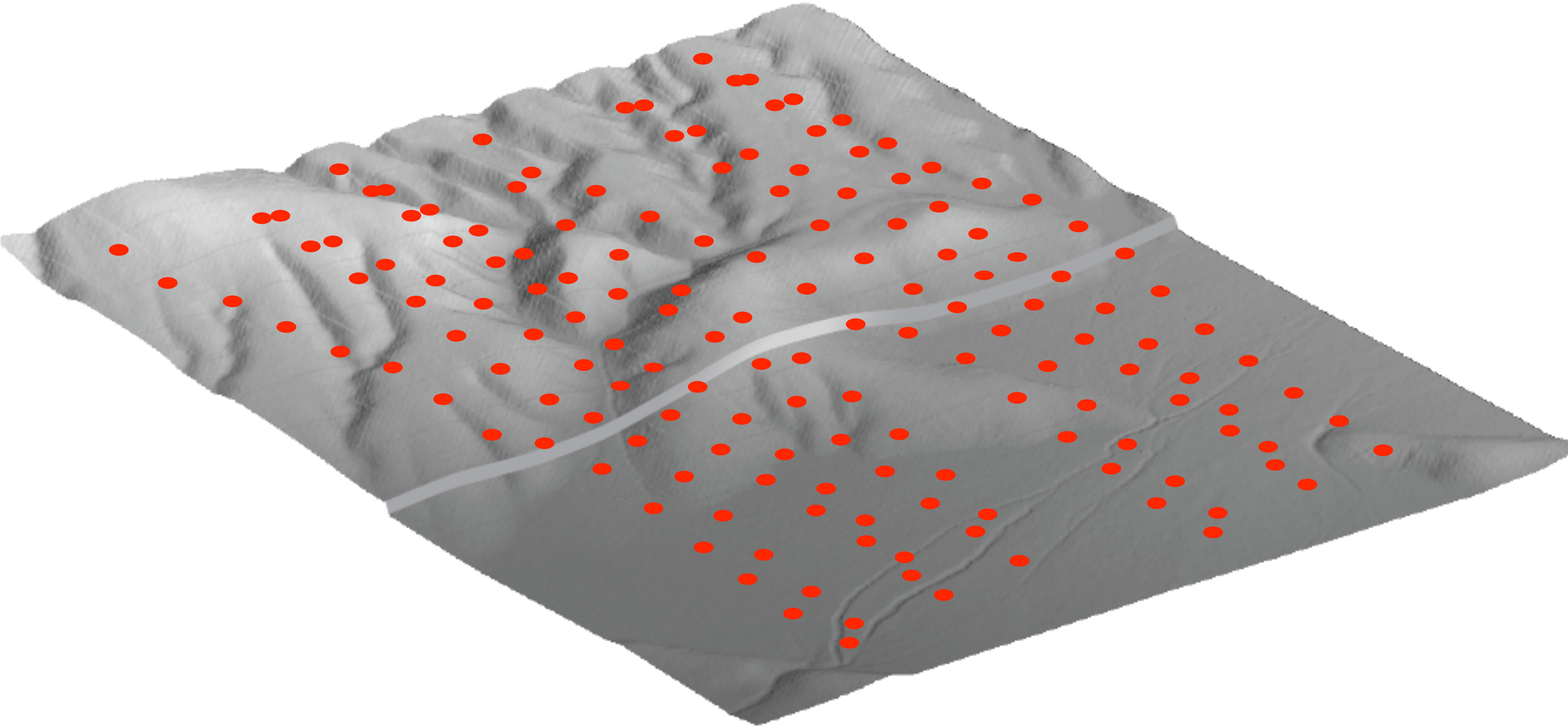

Pre-earthquake point cloud

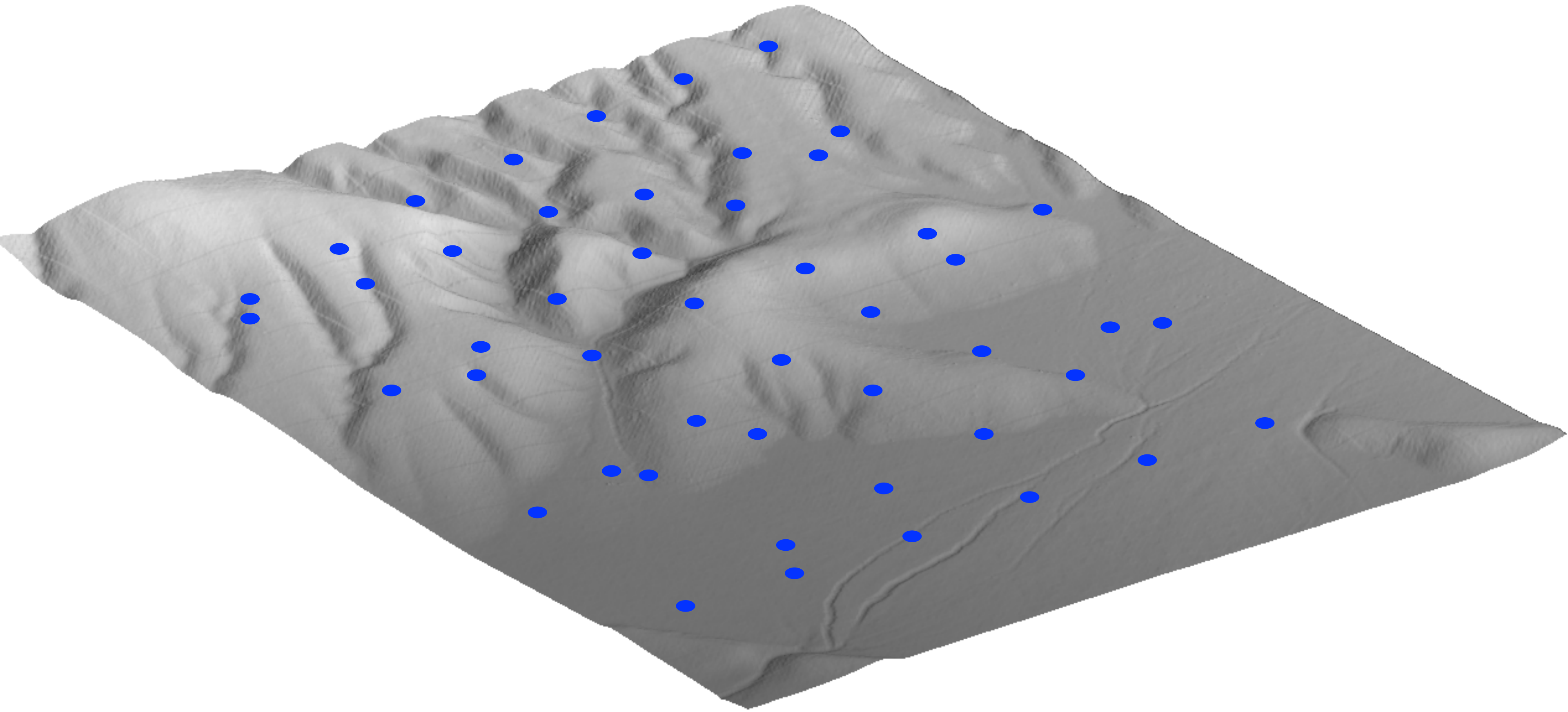

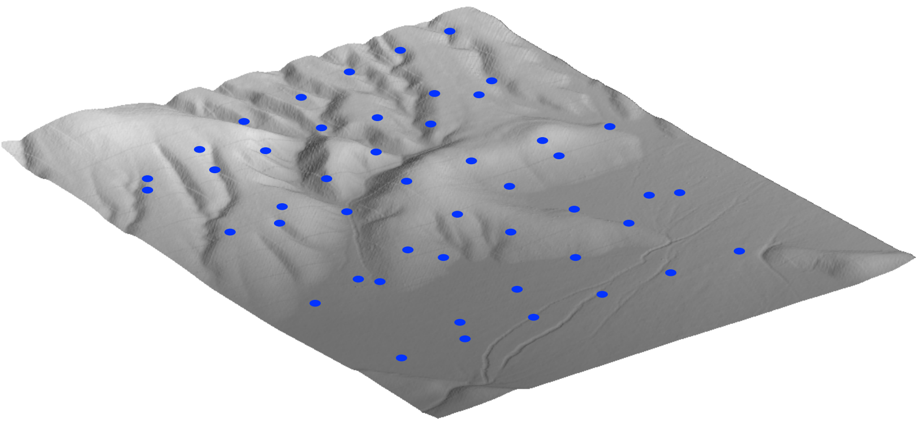

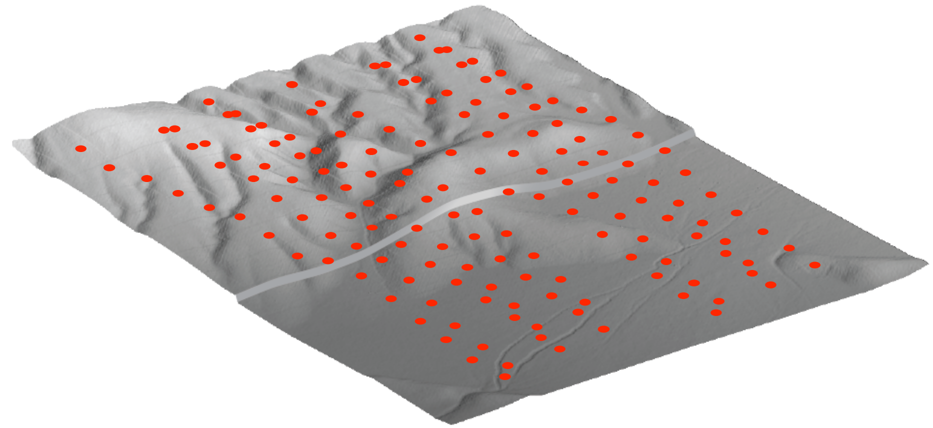

The Challenges of LiDAR differencing

- Data are irregularly spaced
  (we can rasterize them, but we lose information doing so).

- There can be large mismatches in point density
  (typically the newer dataset is denser than the older one).

- There may also be large errors in absolute point positioning
  (for instance at the edges of scan lines, as we saw at El Mayor).

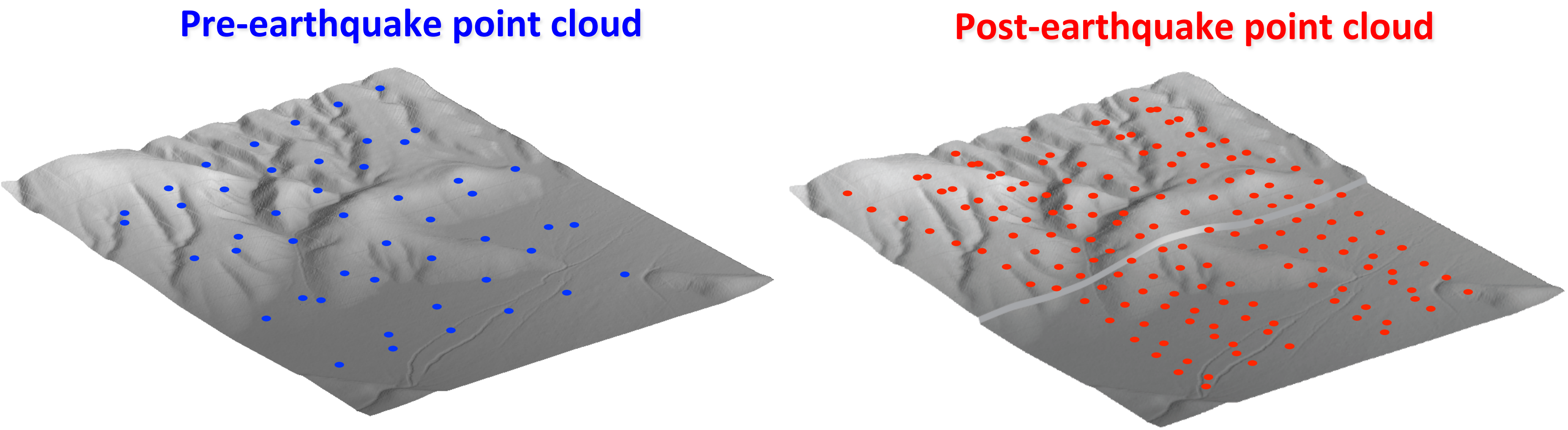

The **Iterative Closest Point** algorithm: a method for registering (aligning) two sets of points

Fig. 4. Iterative point-based registration of phantom face range data

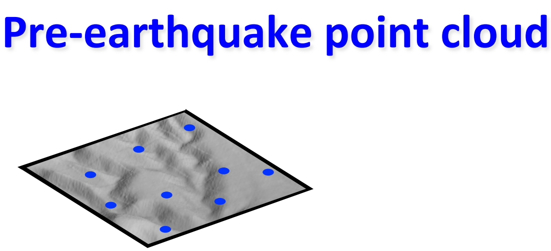

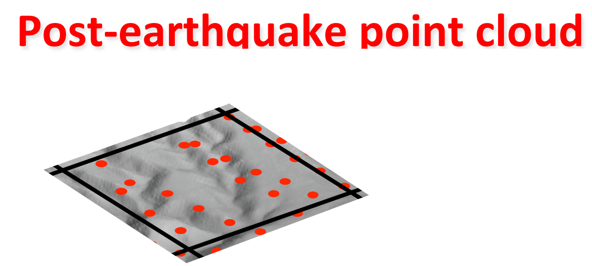

The **Iterative Closest Point** algorithm: a method for registering (aligning) two sets of points

- the two point clouds are first split into square "windows", 50 m in diameter
- ICP is run separately on each pair of windows. (An additional "fringe" of 5 m is included in the post-event window in order to capture the coseismic displacement)
- ICP finds the displacement and rotation that best aligns the pre-event and post-event point clouds.
- This alignment corresponds to the local coseismic displacement for that window.

see Nissen et al. (2012), Geophys. Res. Lett., for details

Pre-earthquake point cloud

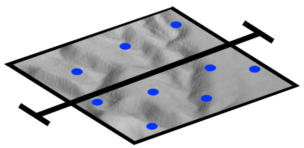

Post-earthquake point cloud

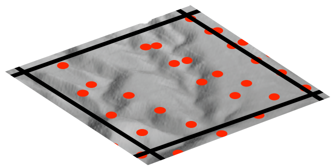

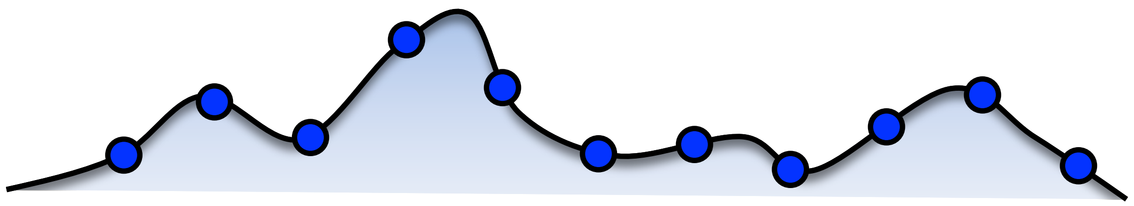

Pre-earthquake point cloud

Post-earthquake point cloud

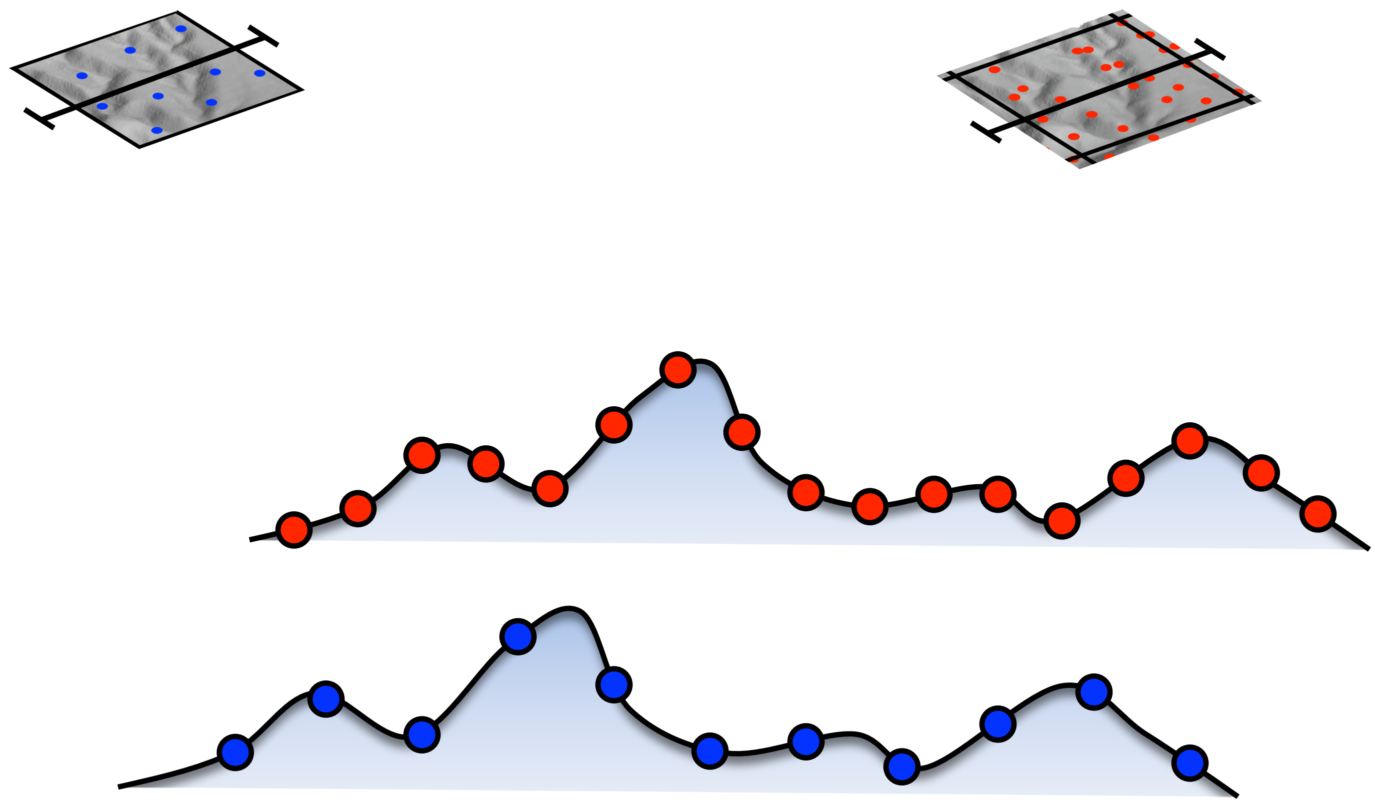

Pre-earthquake point cloud

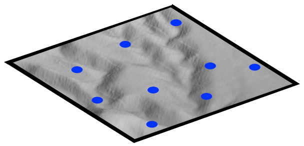

Post-earthquake point cloud

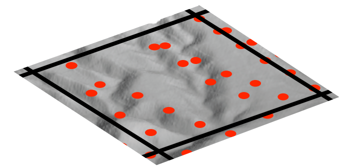

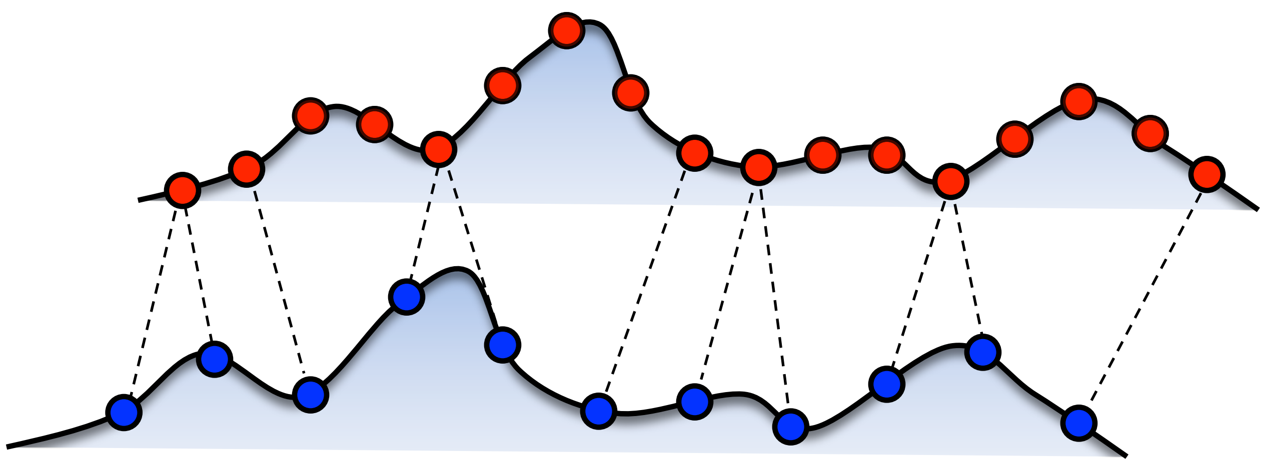

Find closest points

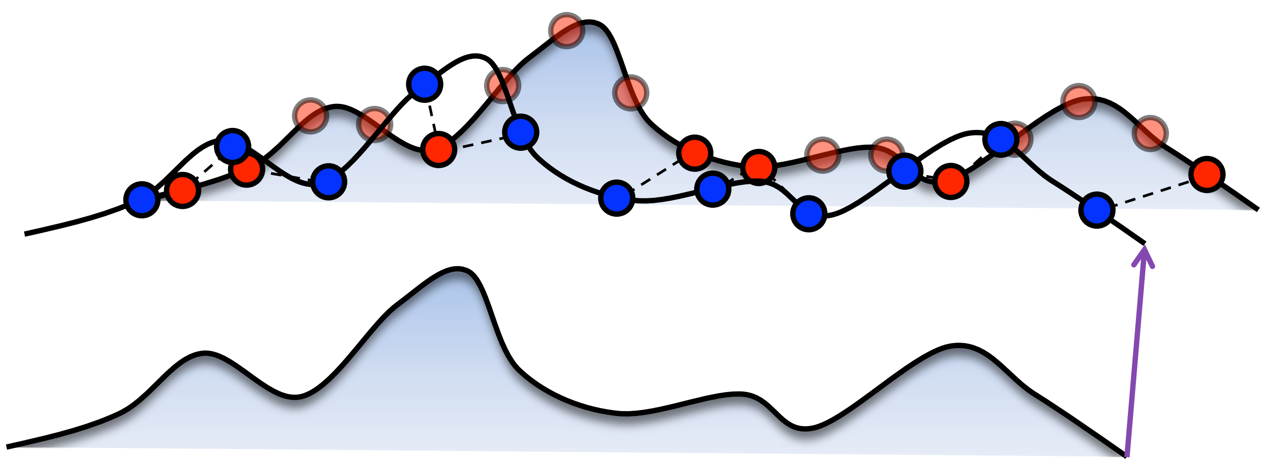

Iterate
Find closest points
Transform point cloud

$$\phi = \begin{pmatrix} 1 & -\gamma & \beta & t_x \\ \gamma & 1 & -\alpha & t_y \\ -\beta & \alpha & 1 & t_z \\ 0 & 0 & 0 & 1 \end{pmatrix}$$

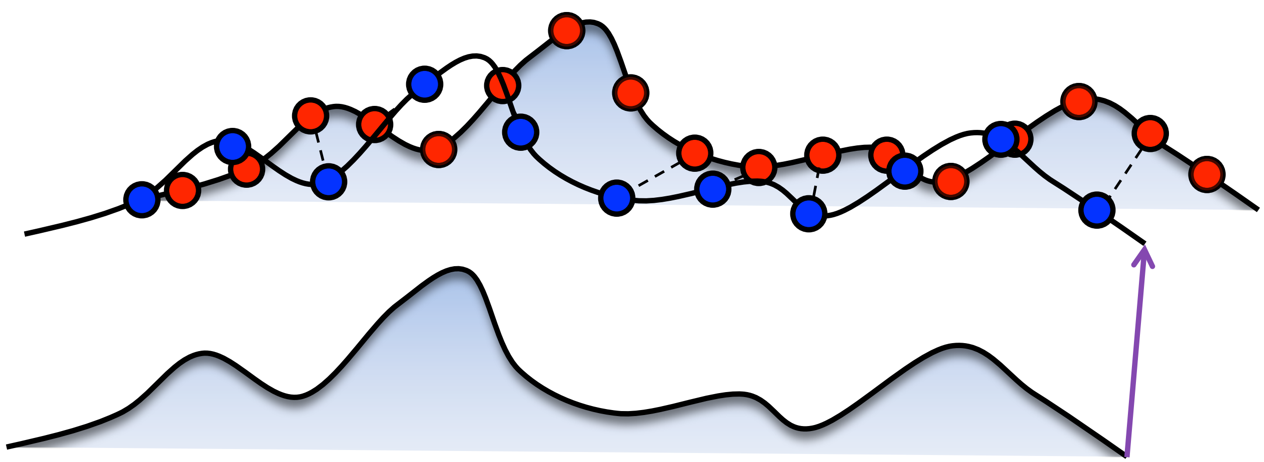

Find closest points

Transform point cloud

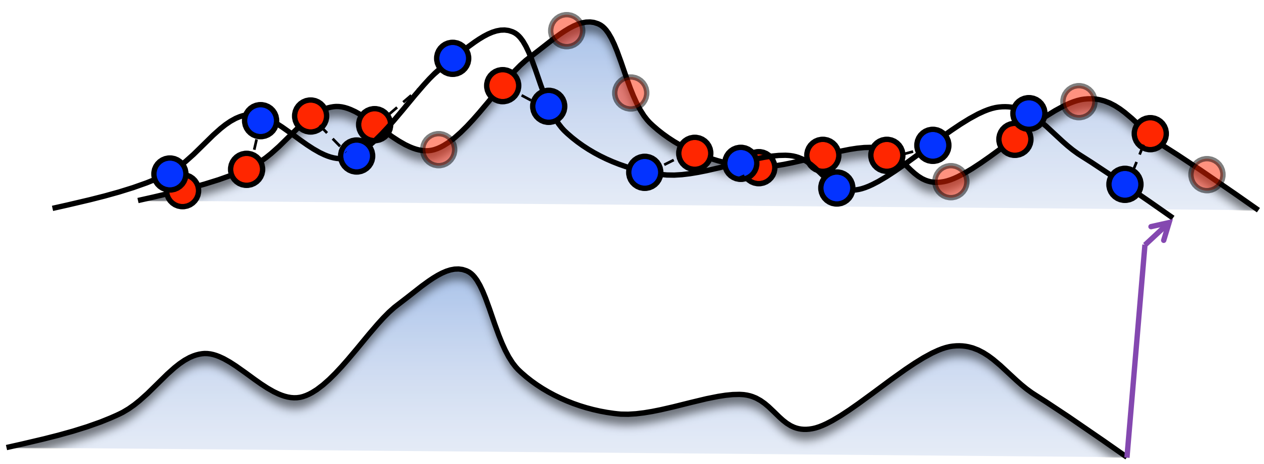

Find closest points

Transform point cloud

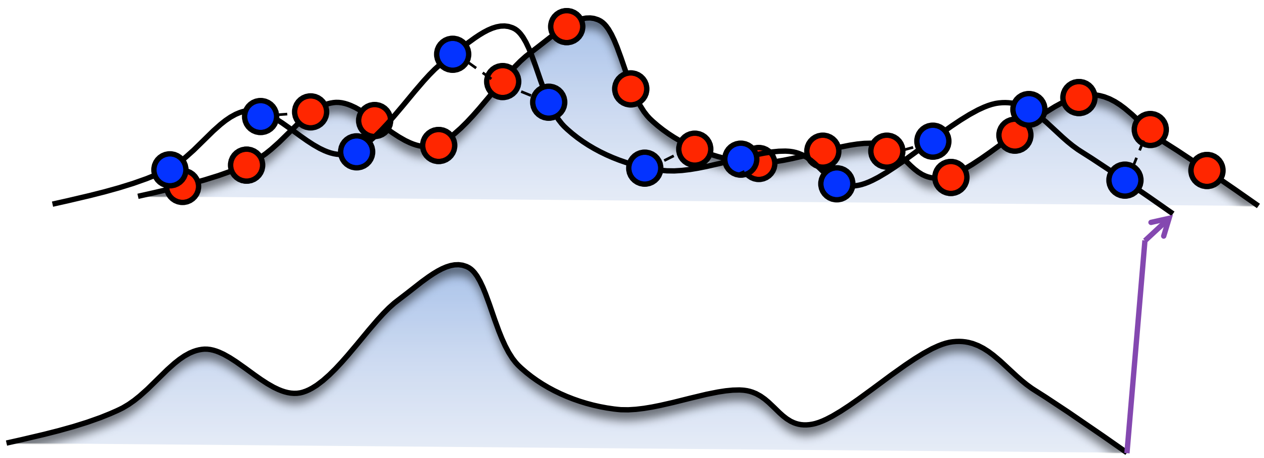

Find closest points

Transform point cloud

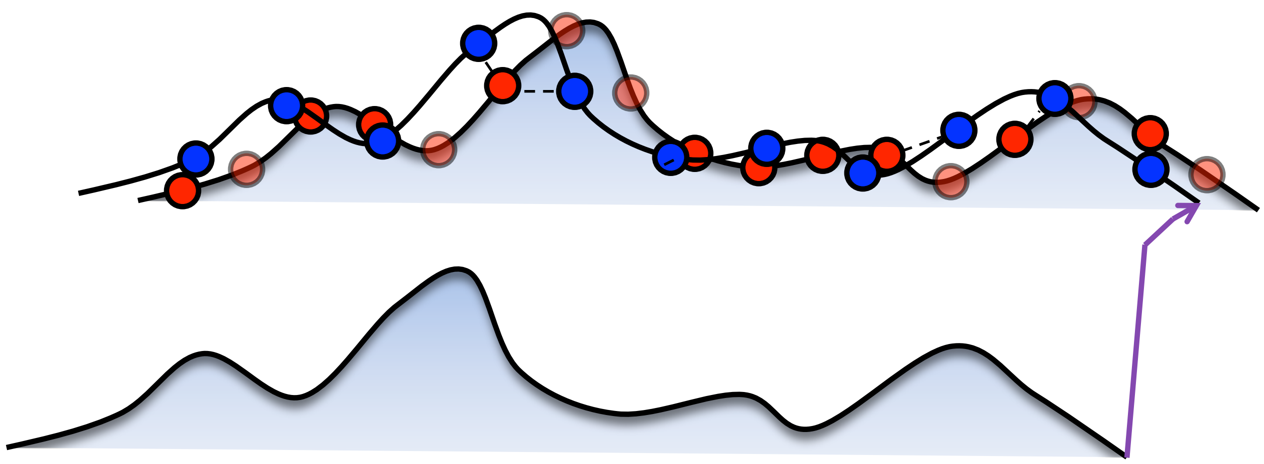

Find closest points

Transform point cloud

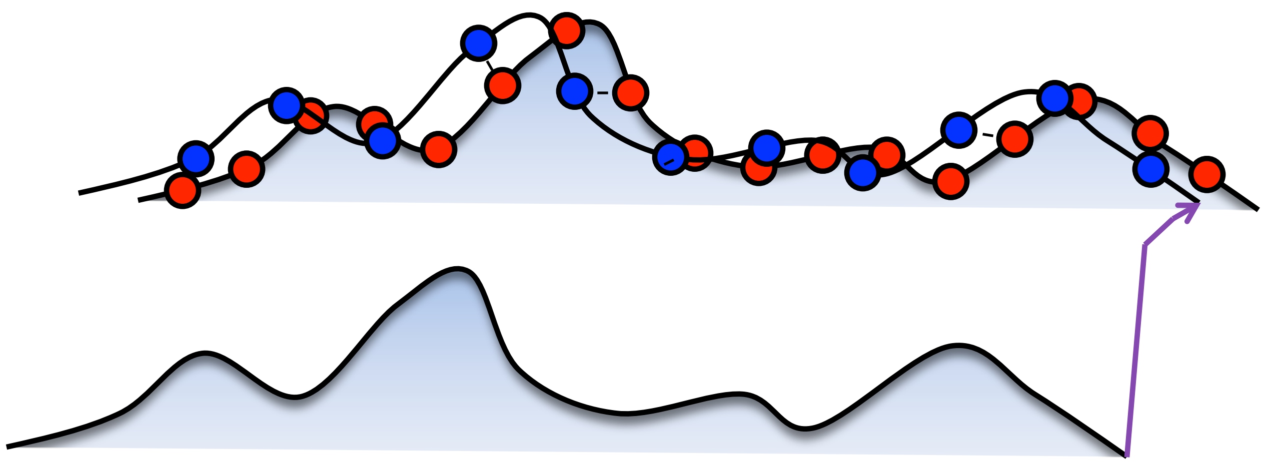

Find closest points

Transform point cloud

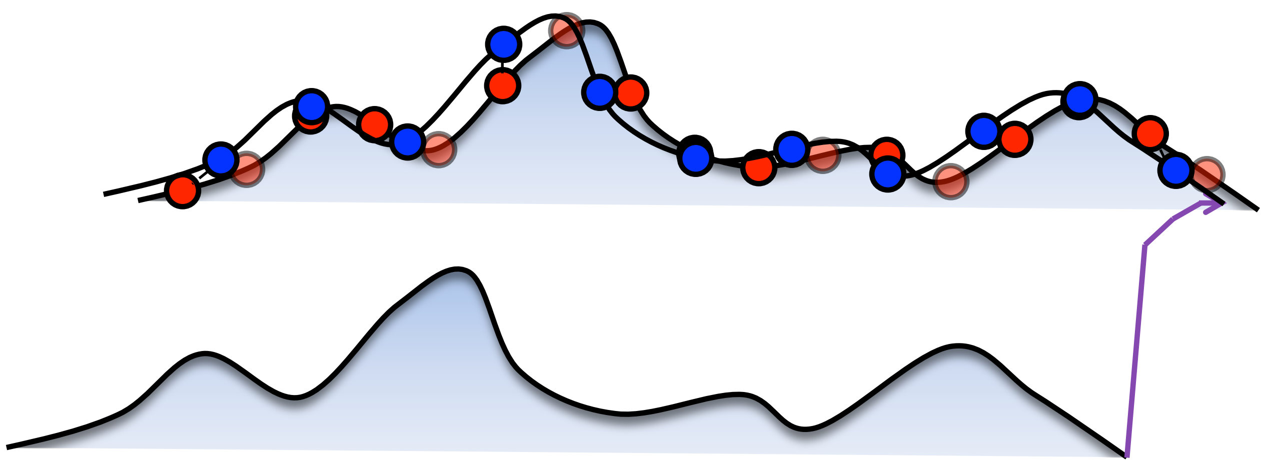

Find closest points

Transform point cloud

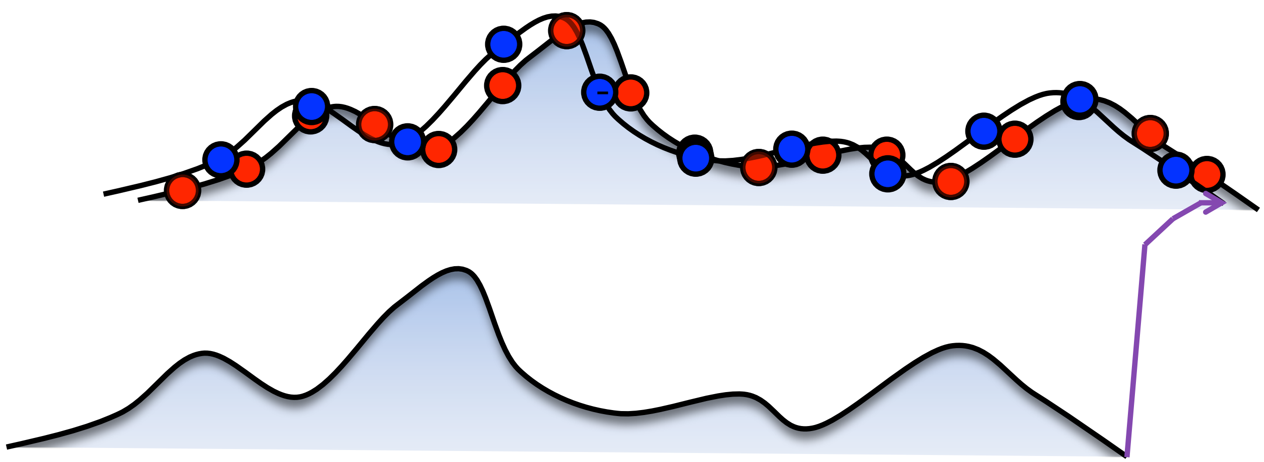

Find closest points

Transform point cloud

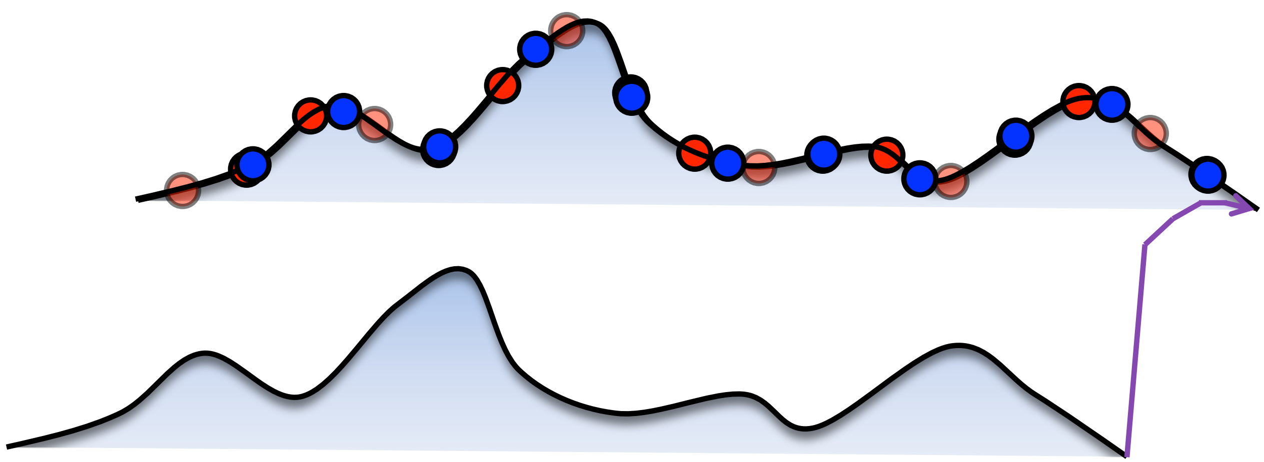

Find closest points

Transform point cloud

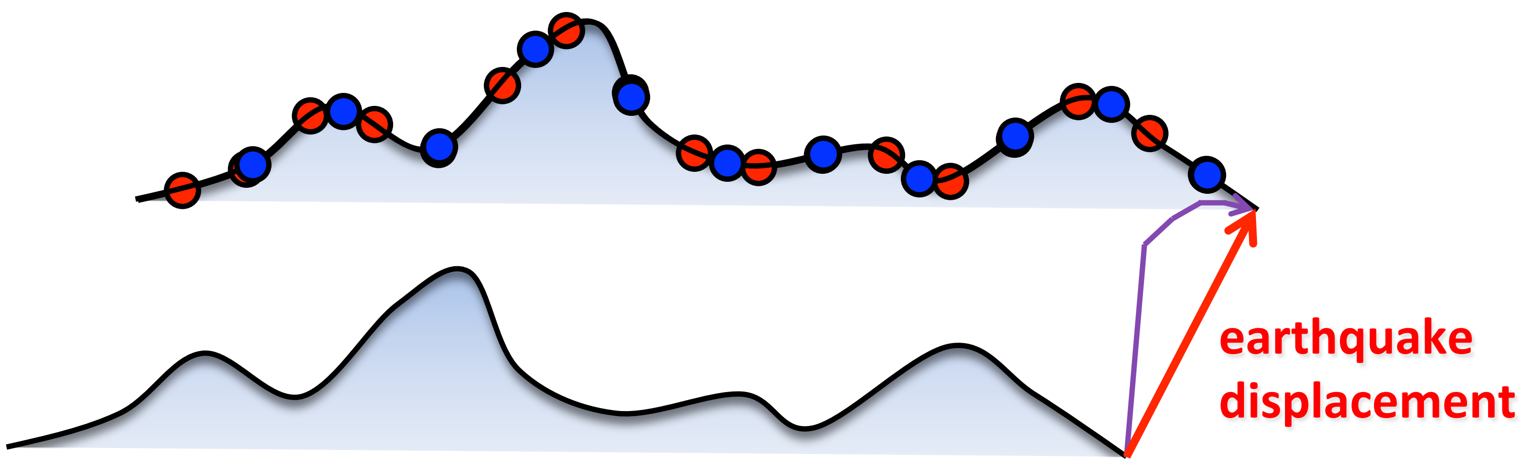

Find closest points

Transform point cloud

Case studies

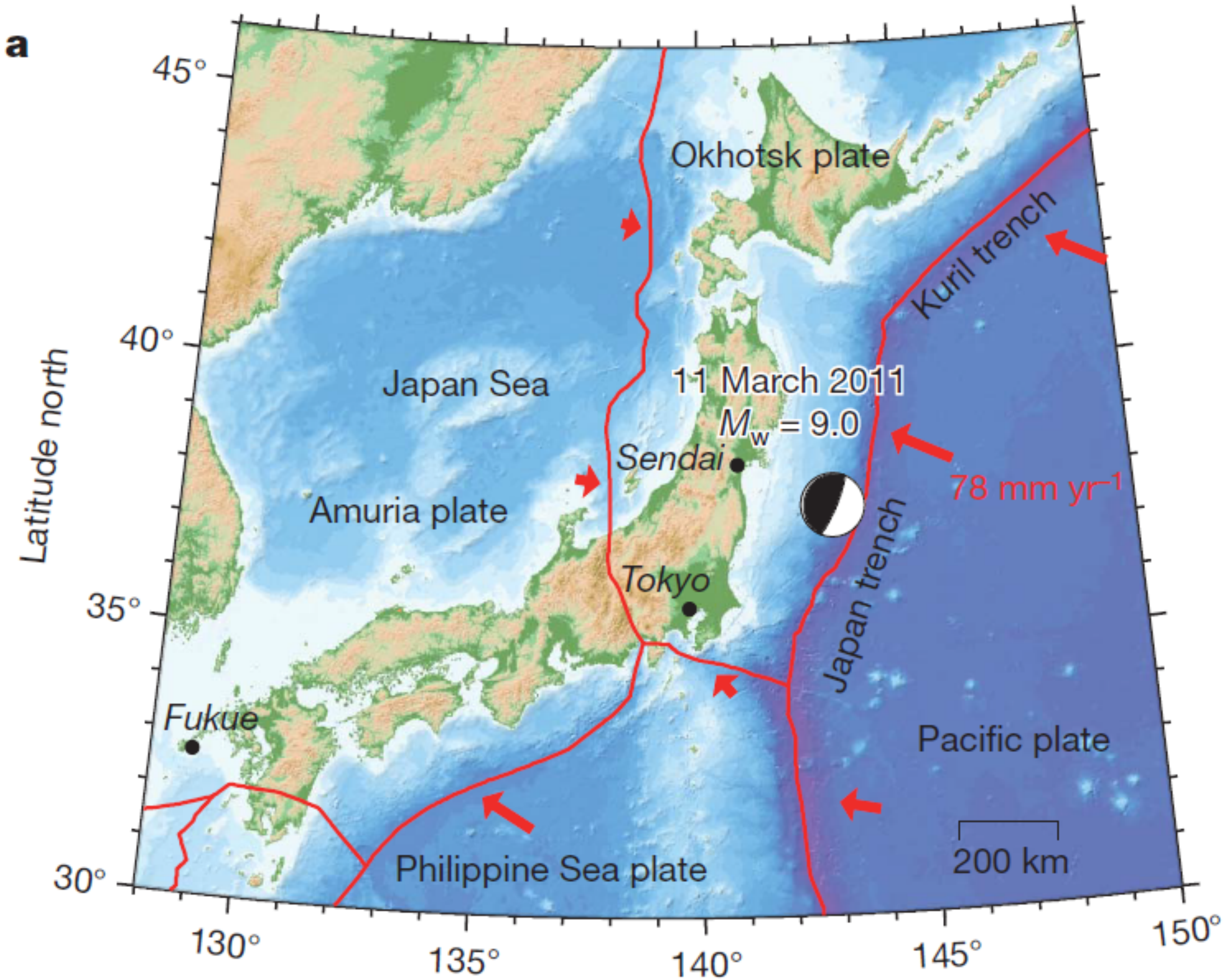

Case studies

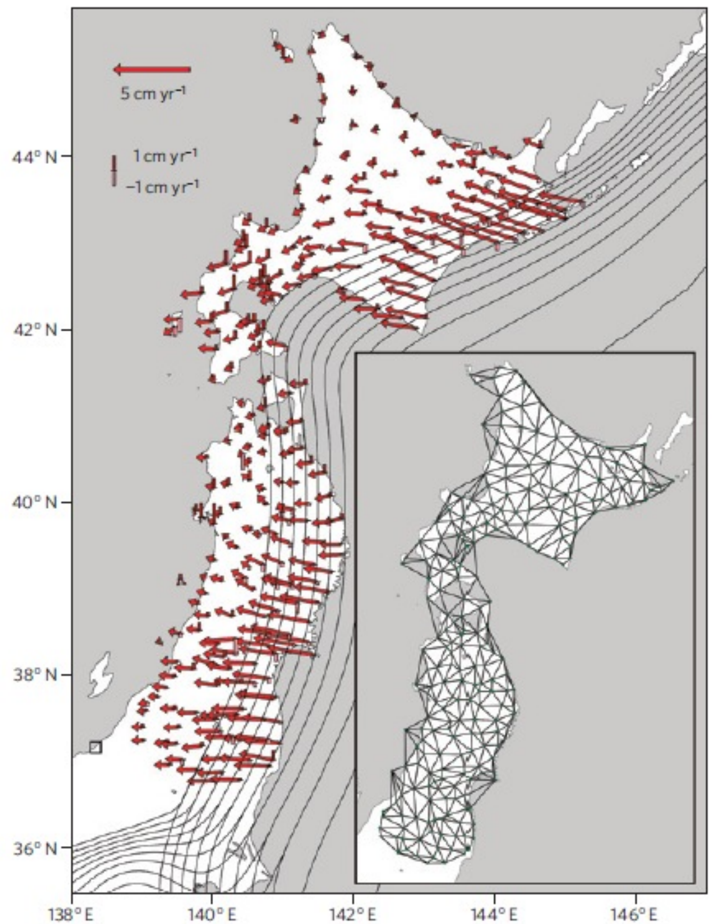

Interseismic GPS velocities, 1996-2000 from Hashimoto et al. (2009)

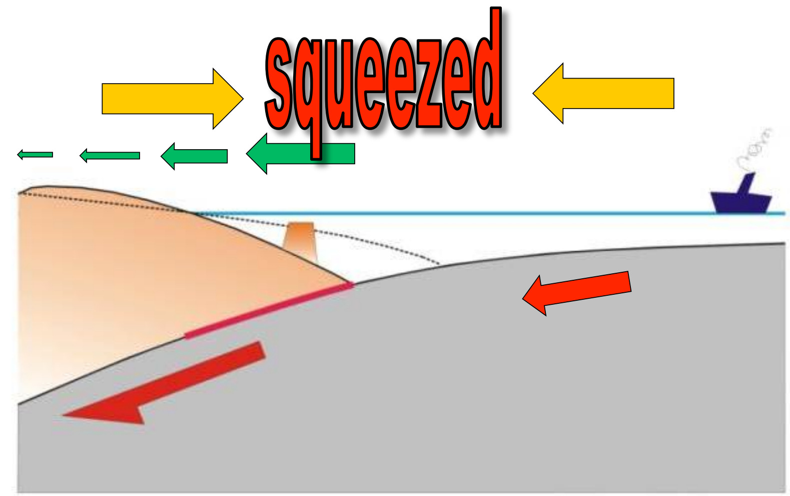

between earthquakes elastic strain accumulates

Case studies

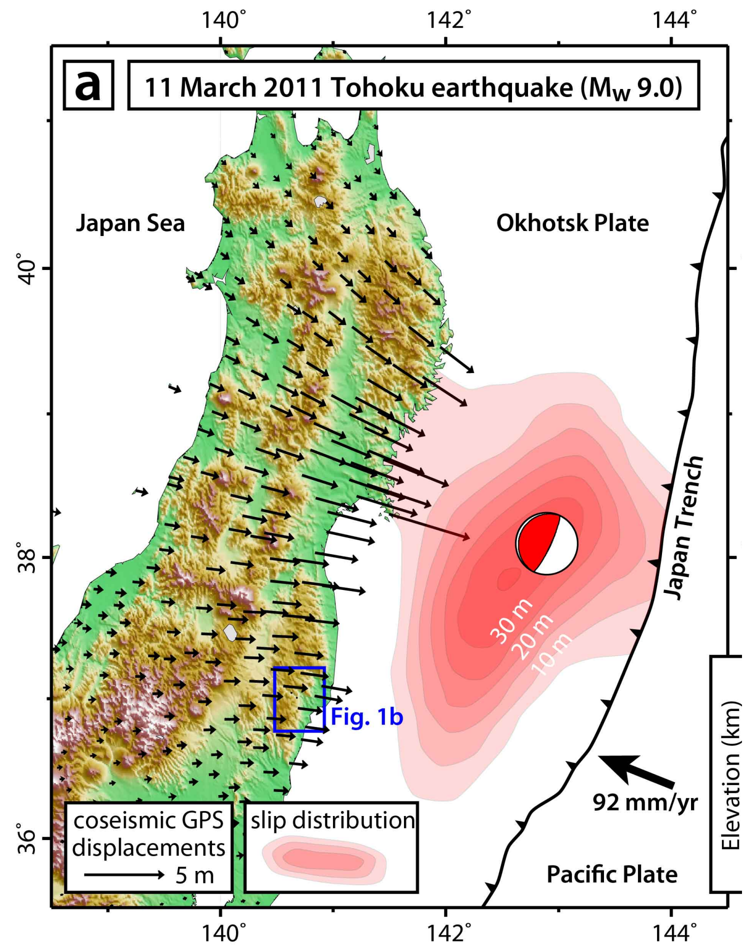

Coseismic GPS velocities from March 11 2011 from Ozawa et al. (2011)

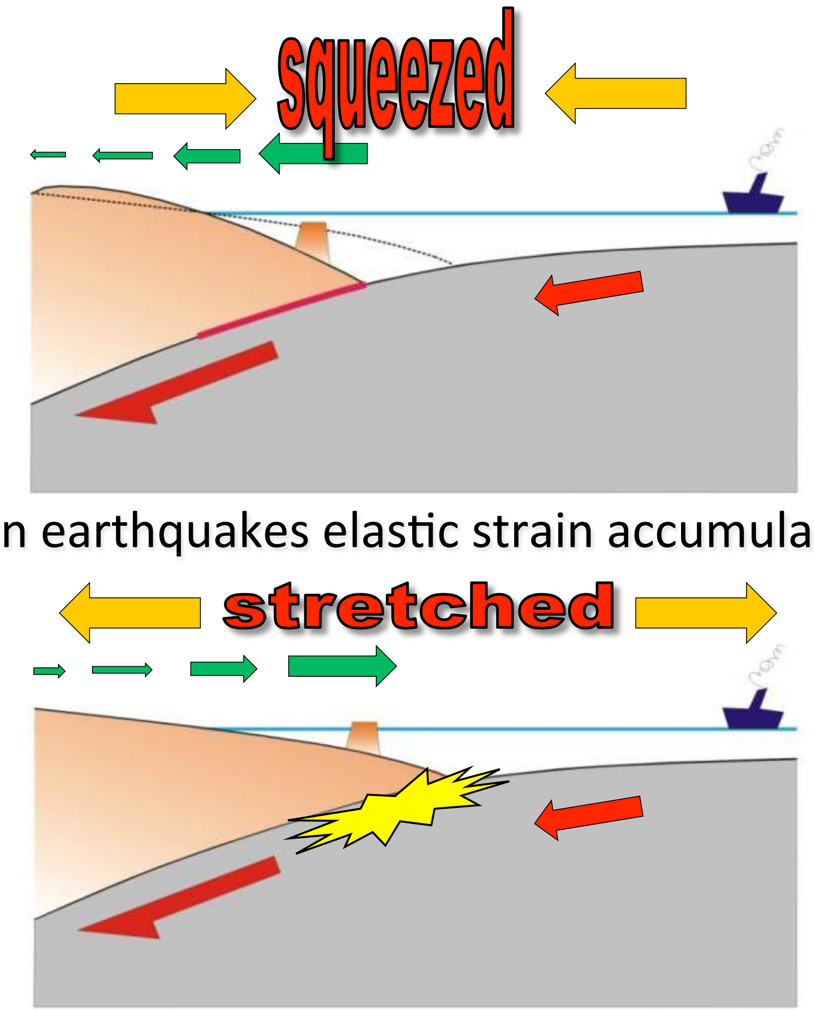

between earthquakes elastic strain accumulates

during earthquake elastic strain is released

Case studies

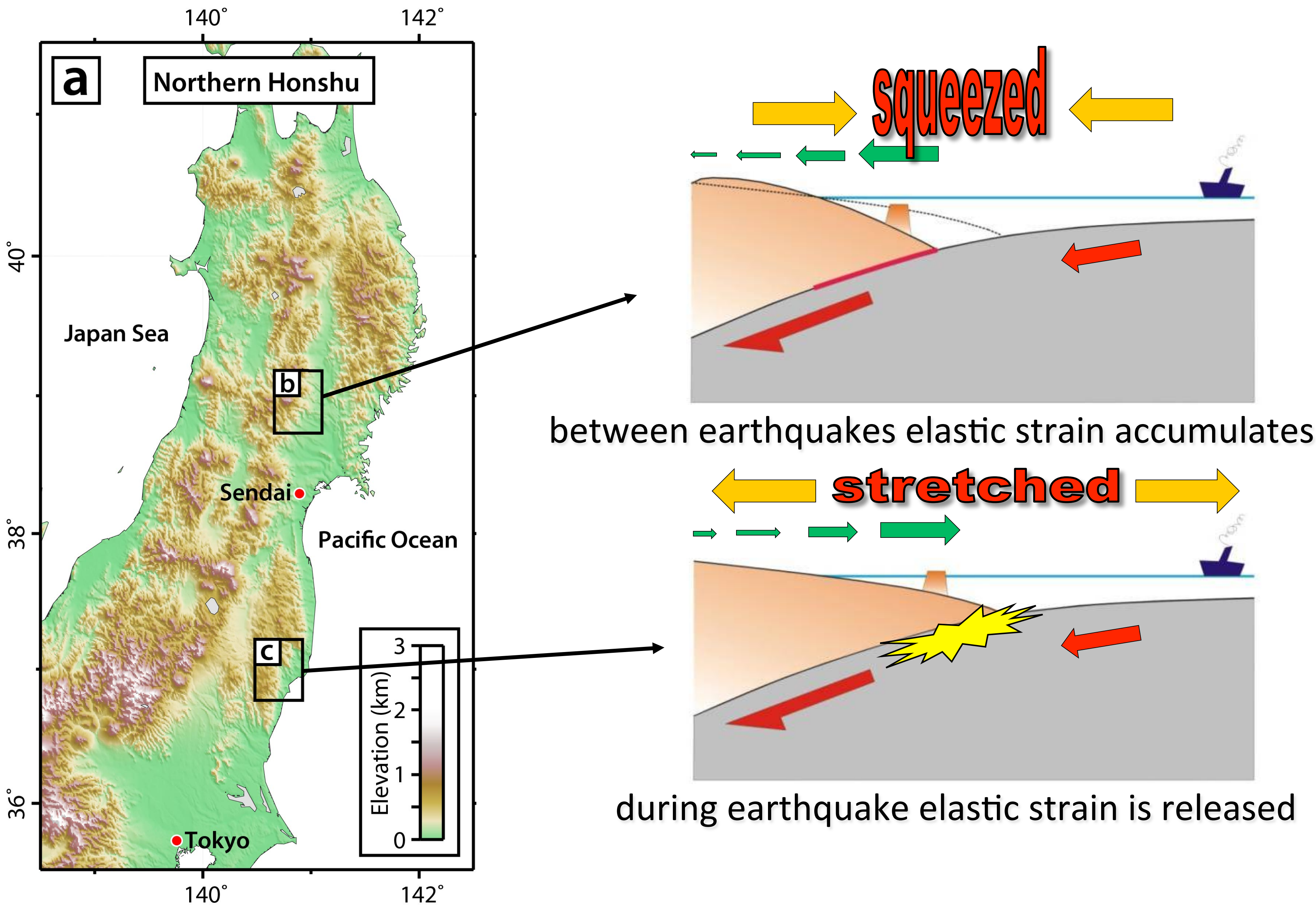

The 2008 Iwate-Miyagi earthquake (Mw 6.9), Japan

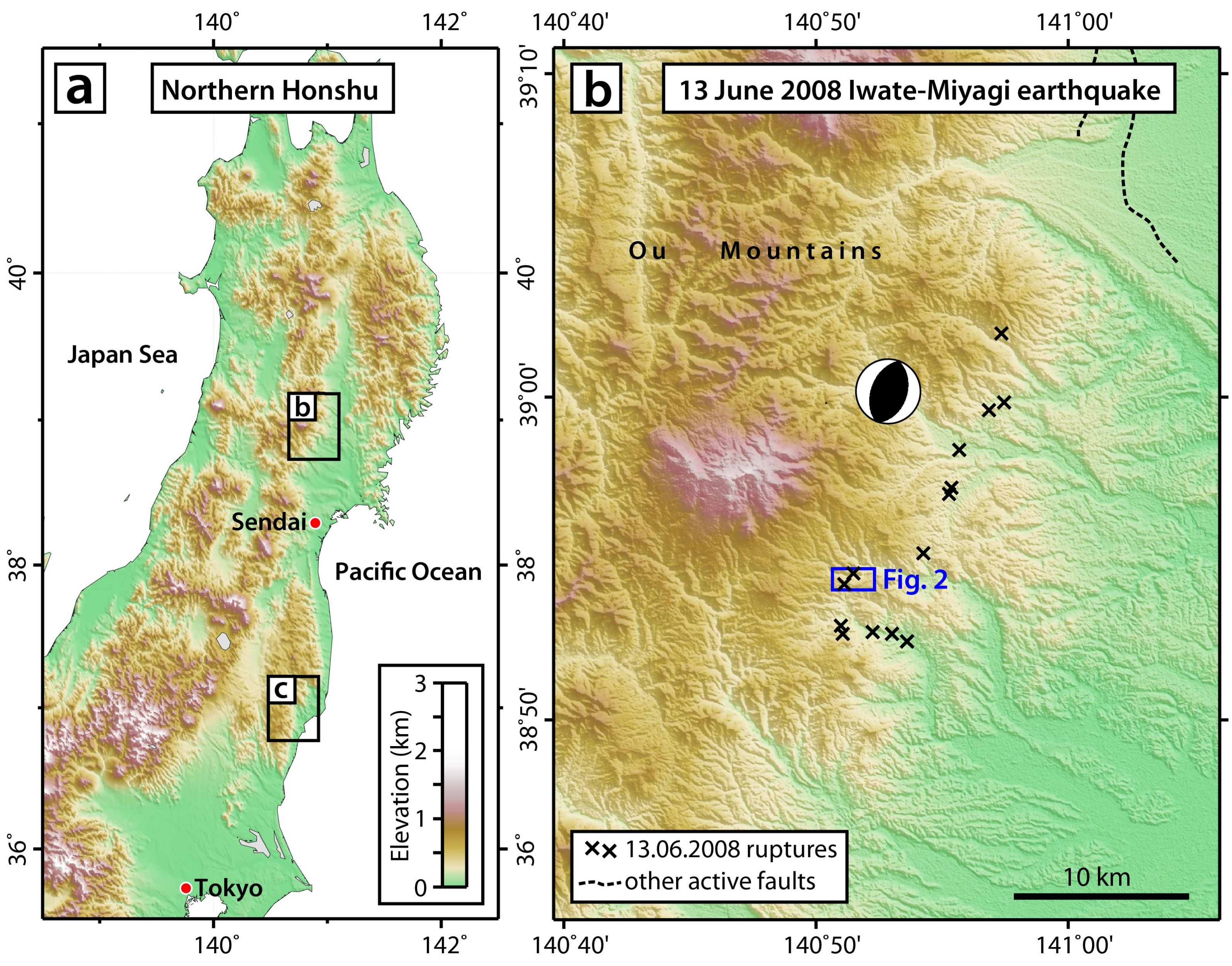

The 2008 Iwate-Miyagi earthquake (Mw 6.9), Japan

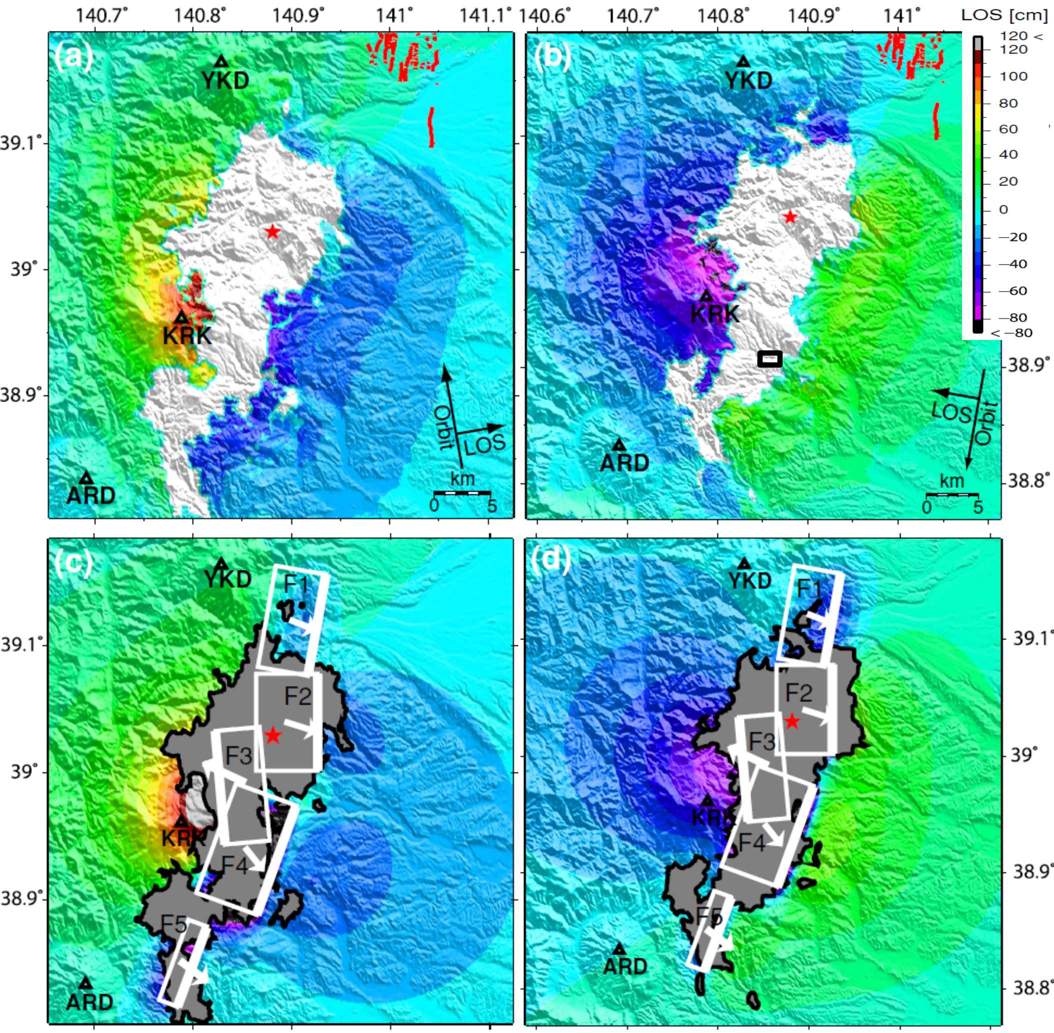

Takada et al. (2009), Earth Planets Space

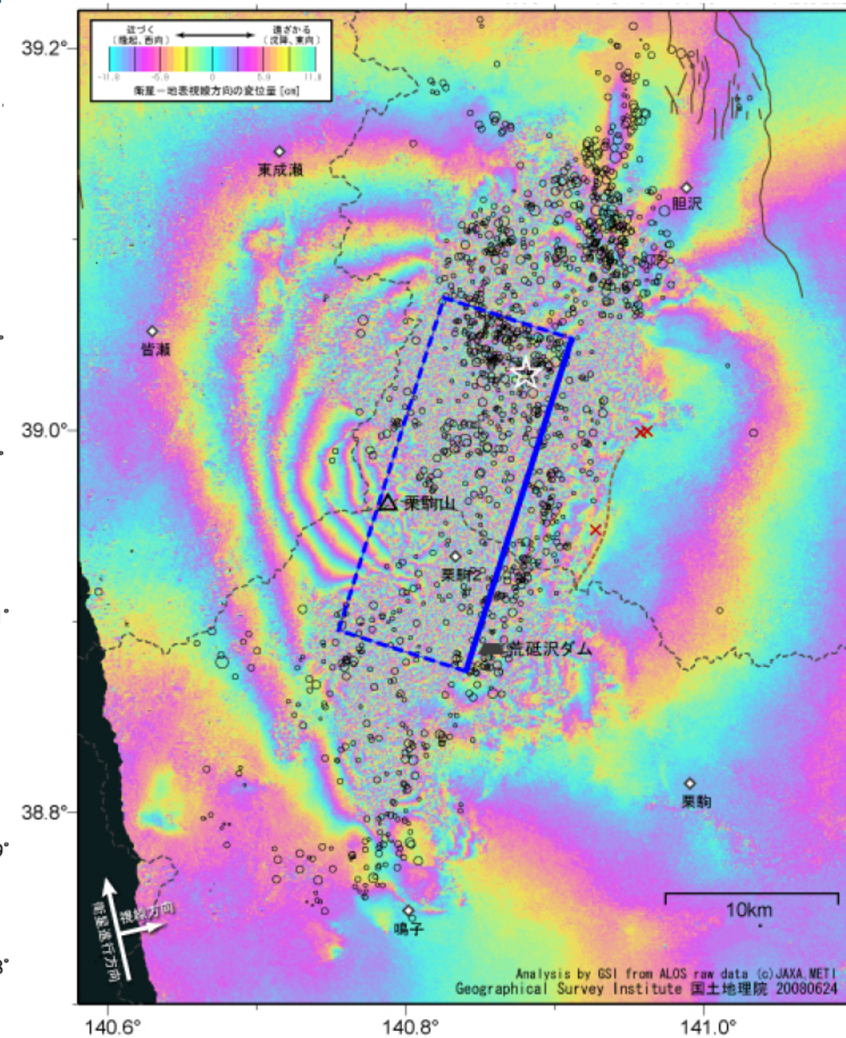

Japan Geographical Survey Institute

The 2008 Iwate-Miyagi earthquake (Mw 6.9), Japan

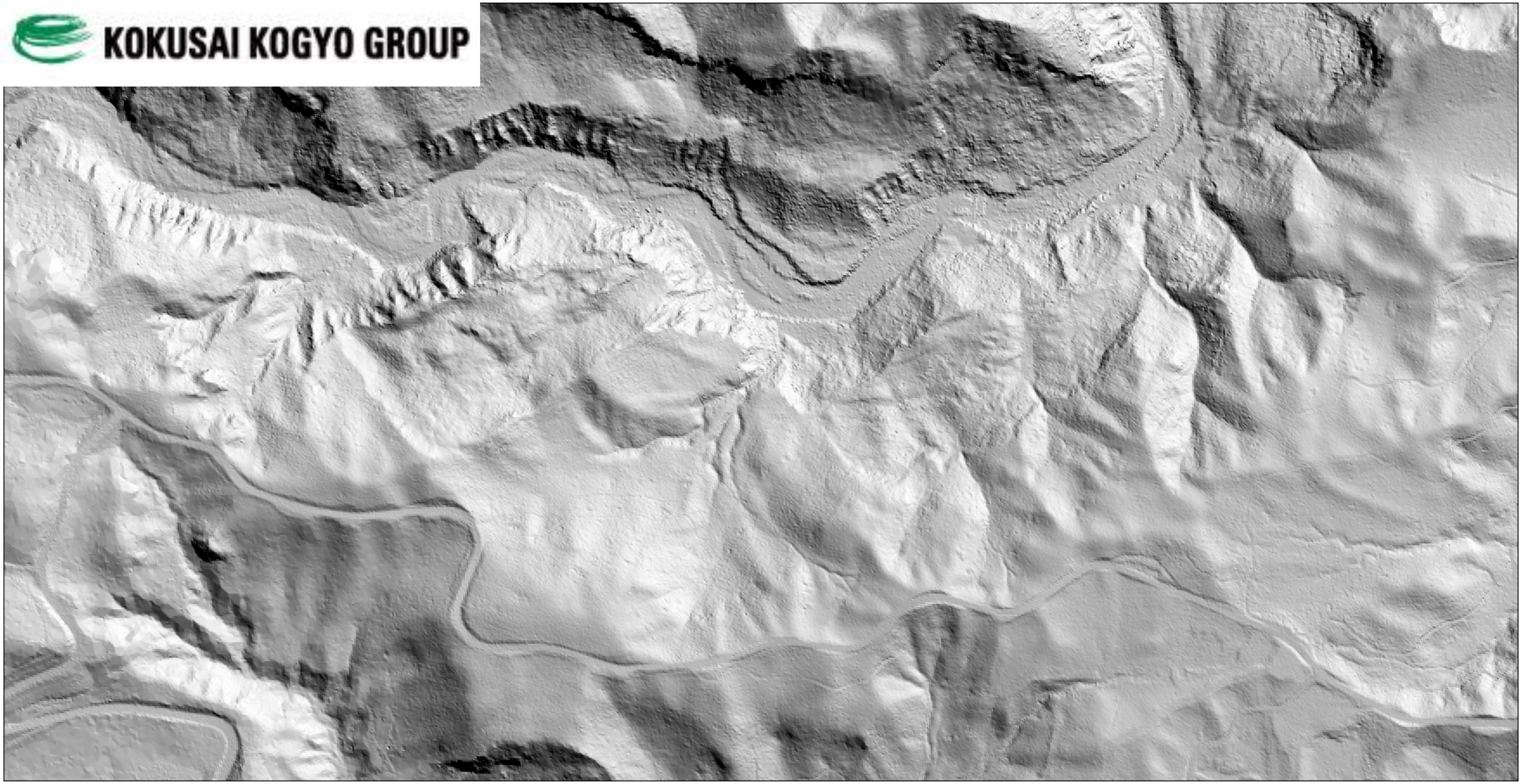

Pre-earthquake DEM (2m)

The 2008 Iwate-Miyagi earthquake (Mw 6.9), Japan

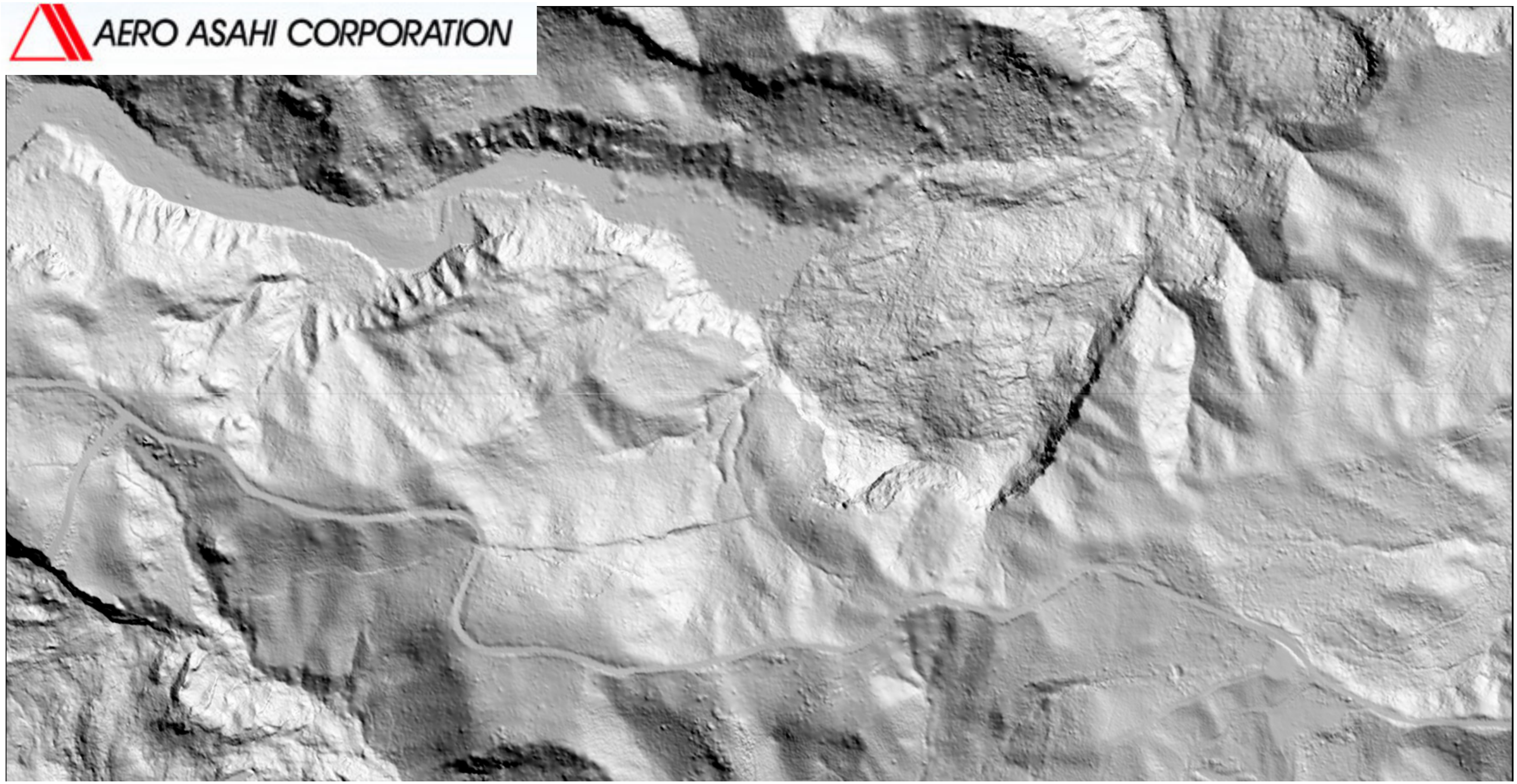

Post-earthquake DEM (1m)

The 2008 Iwate-Miyagi earthquake (Mw 6.9), Japan

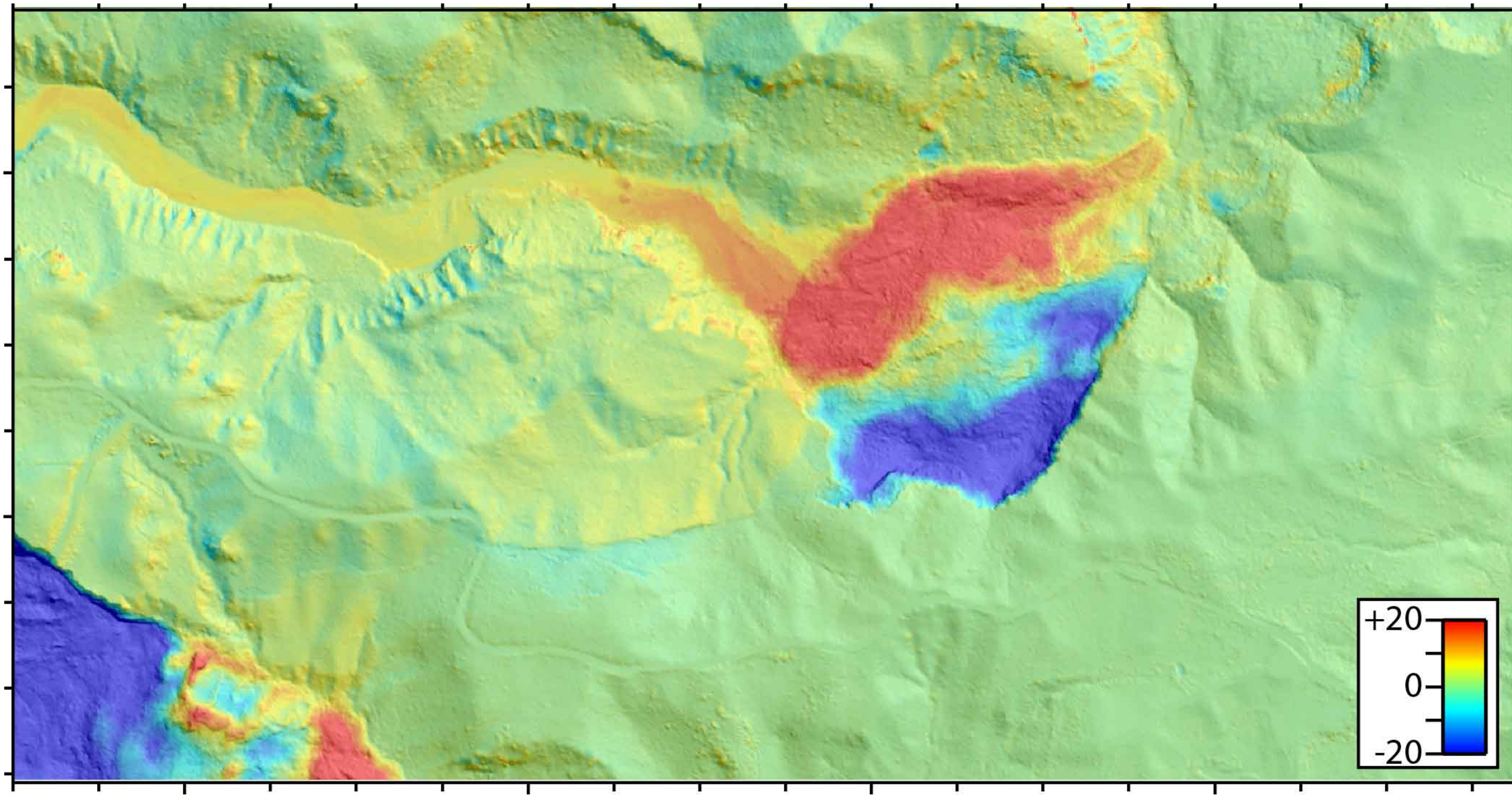

DEM subtraction (height change, m)

The 2008 Iwate-Miyagi earthquake (Mw 6.9), Japan

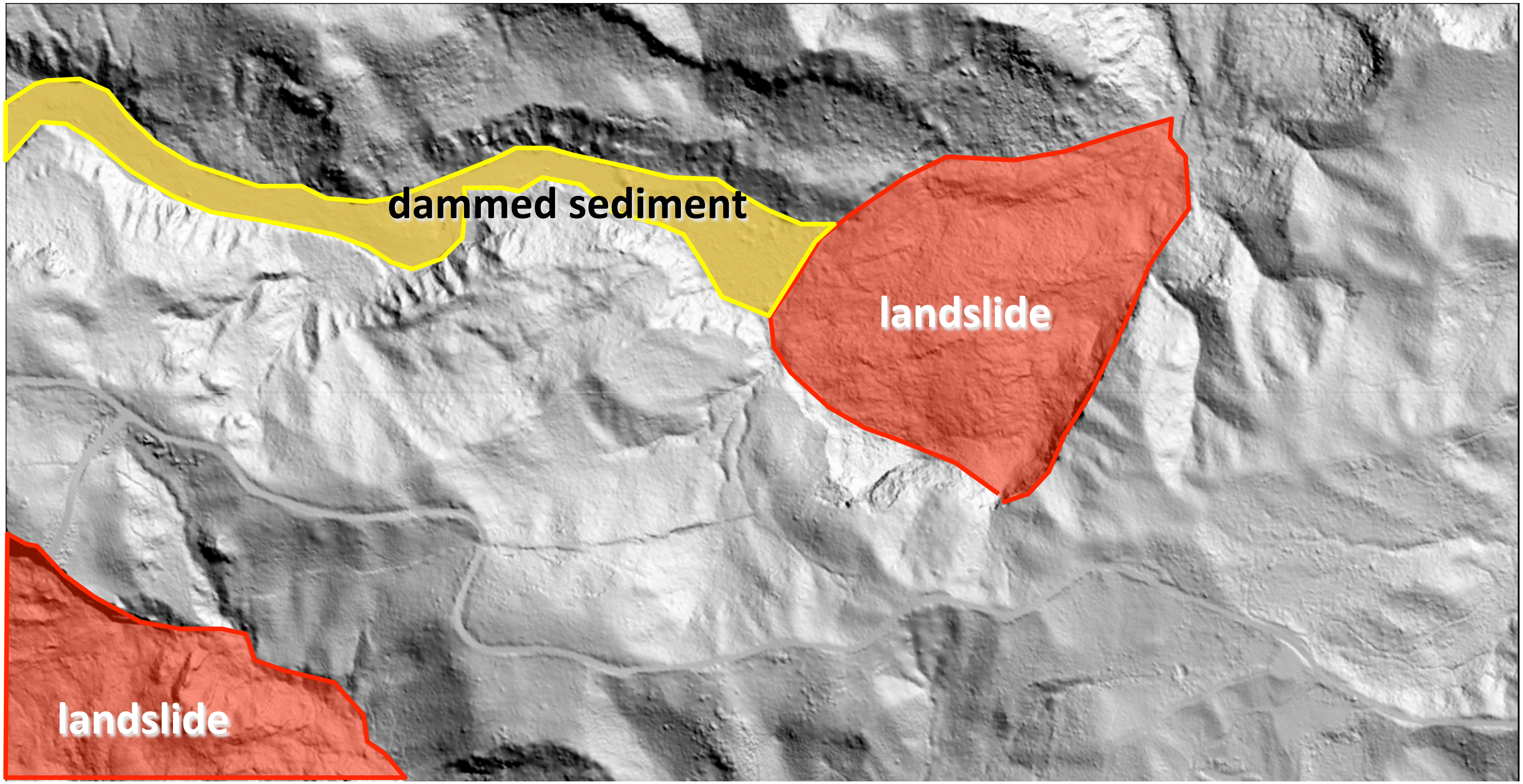

The 2008 Iwate-Miyagi earthquake (Mw 6.9), Japan

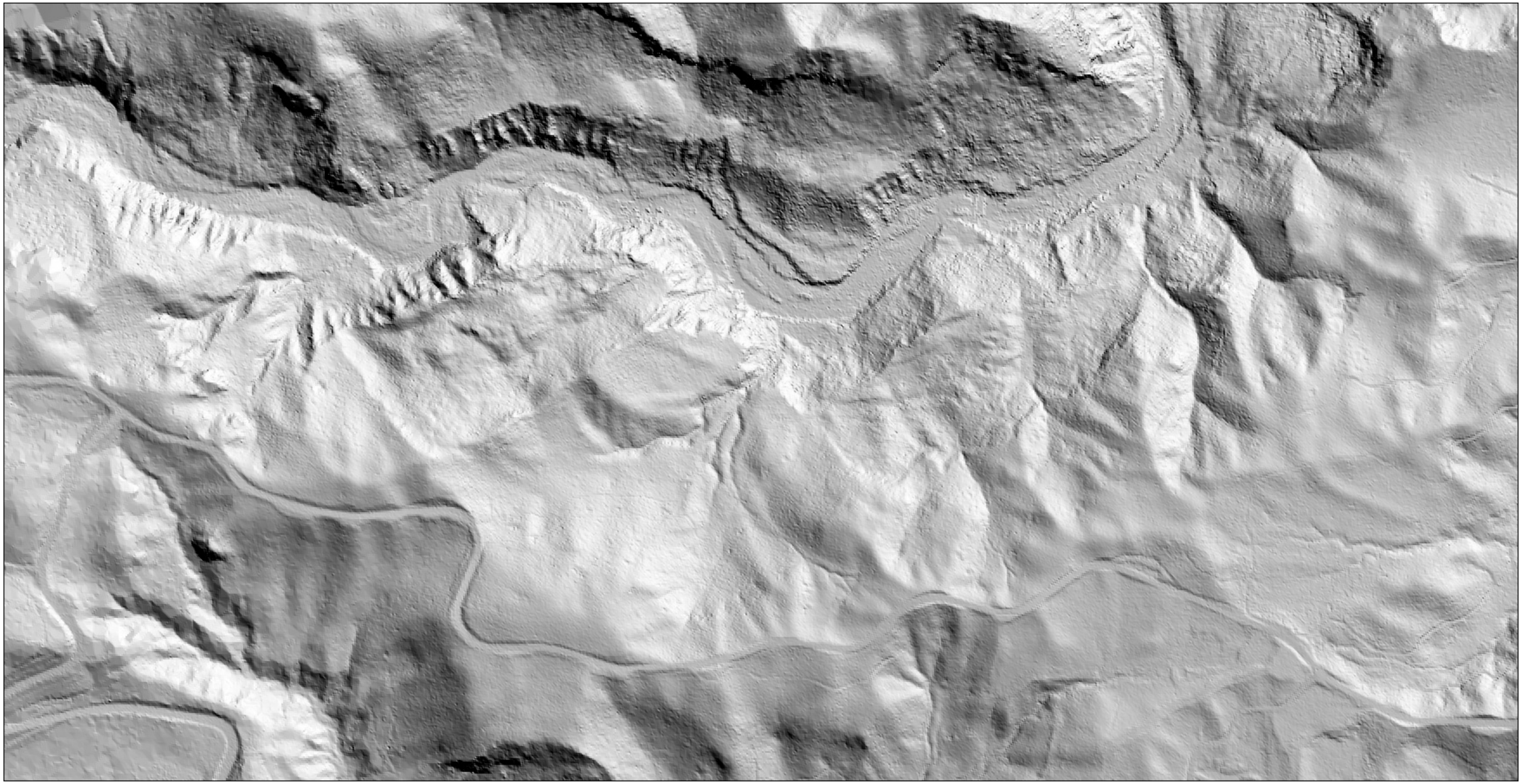

Pre-earthquake DEM (2m)

The 2008 Iwate-Miyagi earthquake (Mw 6.9), Japan

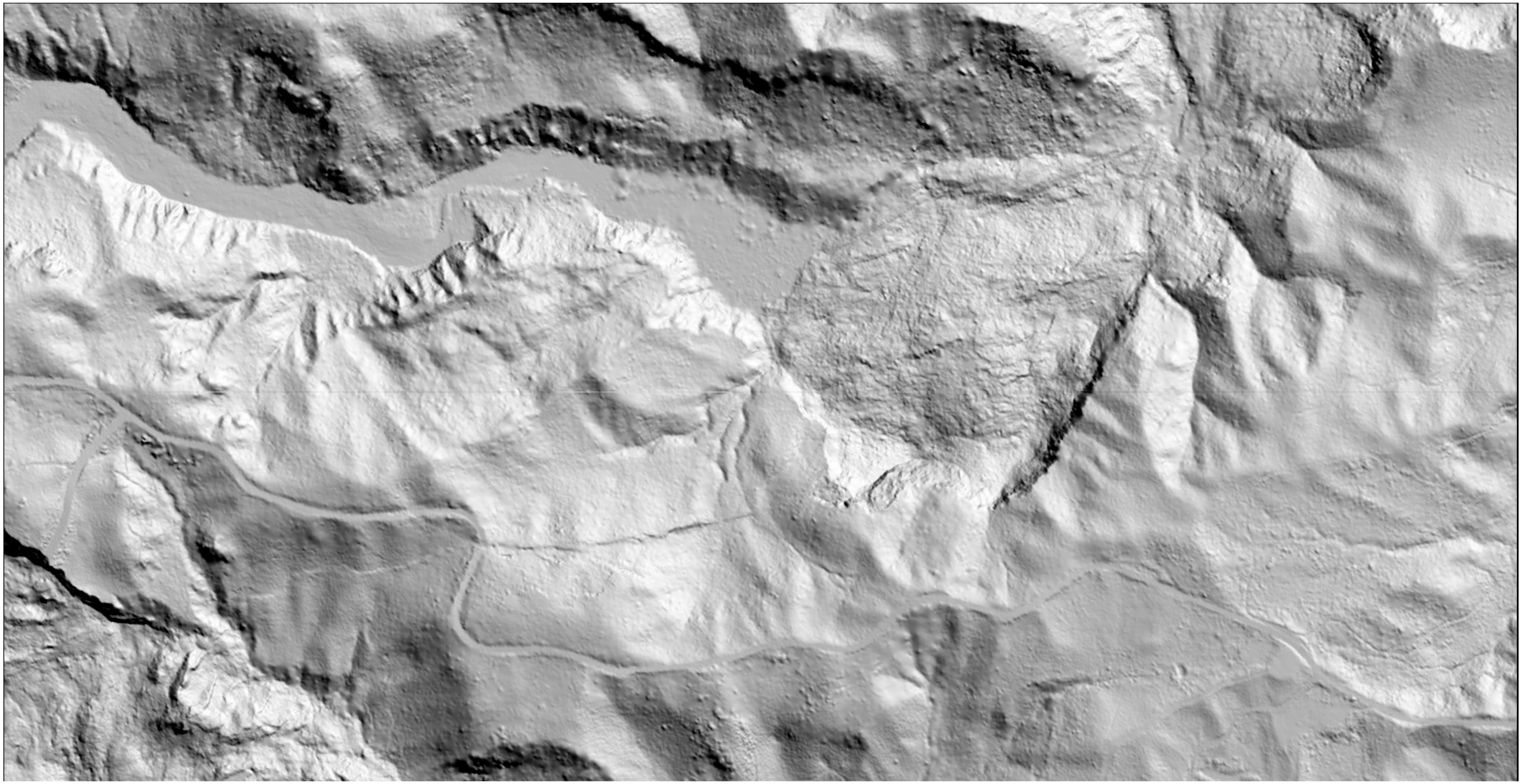

Post-earthquake DEM (1m)

The 2008 Iwate-Miyagi earthquake (Mw 6.9), Japan

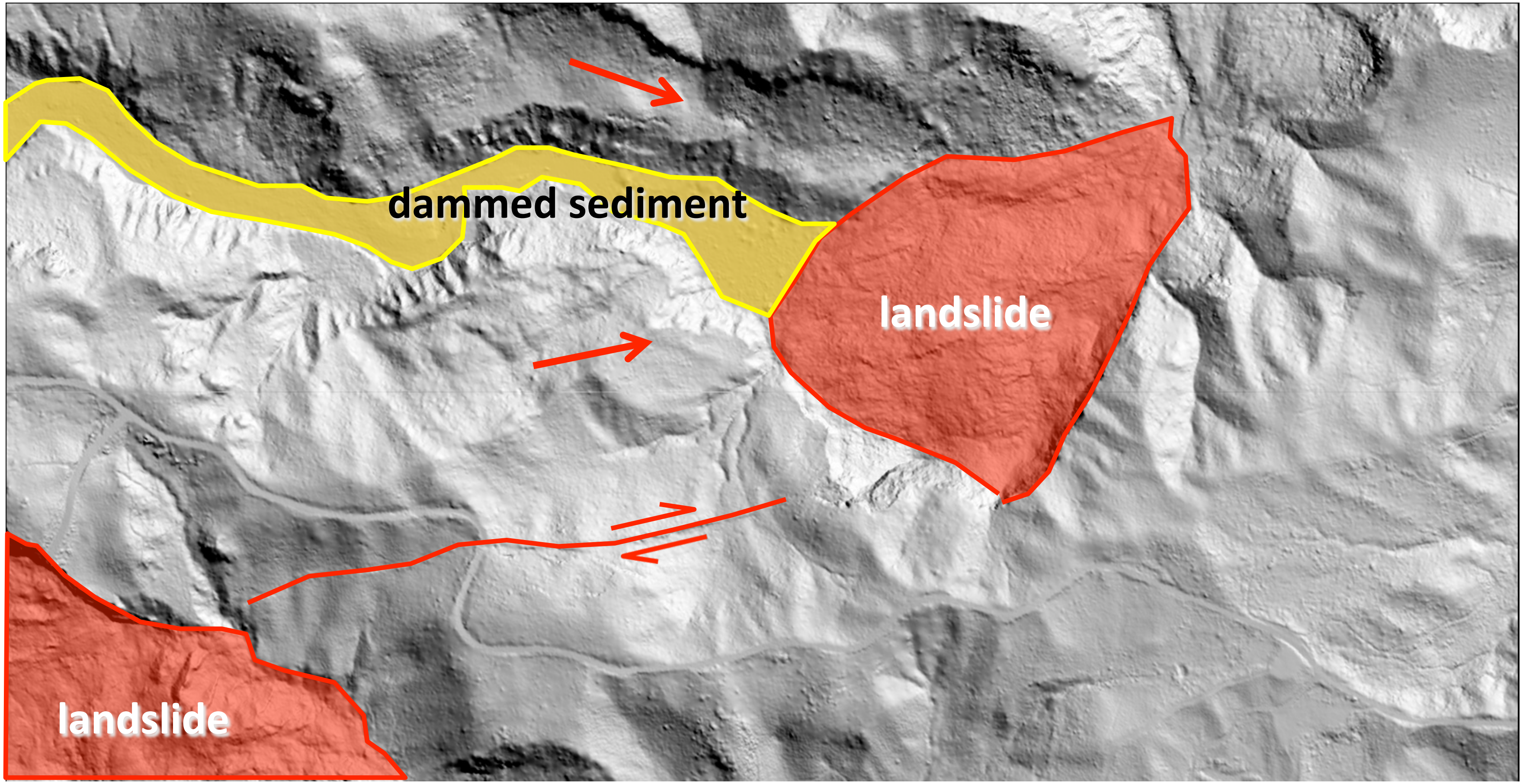

The 2008 Iwate-Miyagi earthquake (Mw 6.9), Japan

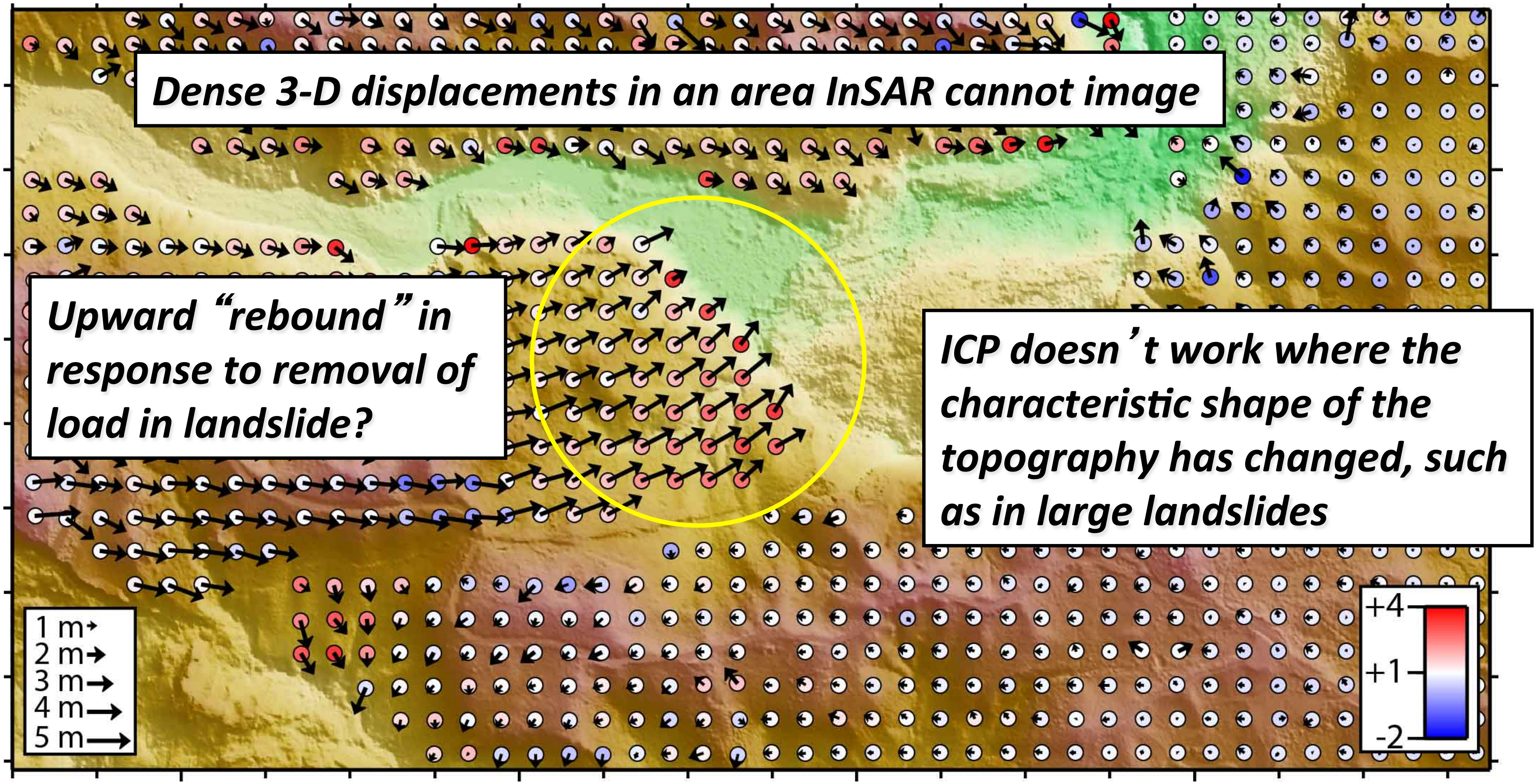

quake (Mw 6.9), Japan

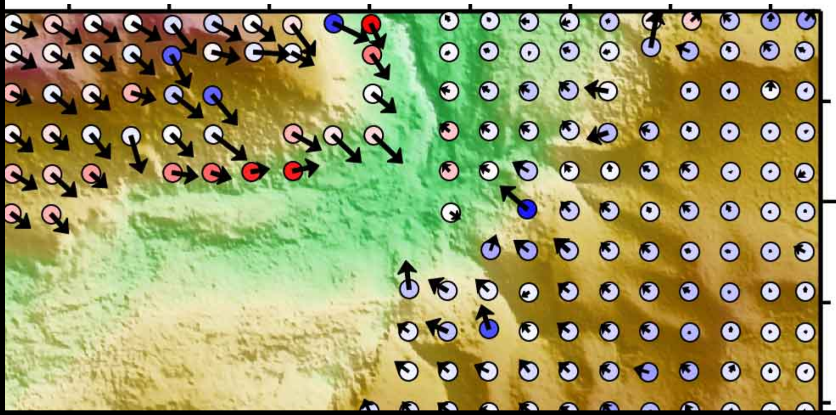

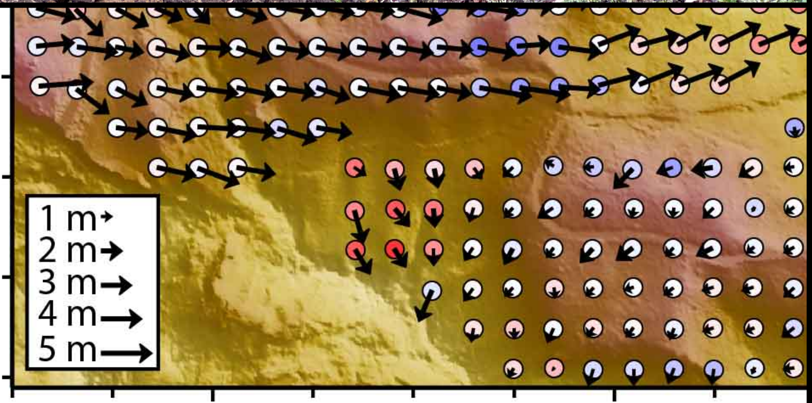

Photos by Tadashi Maruyama

The 2011 Iwaki earthquake (Mw 6.7), Japan

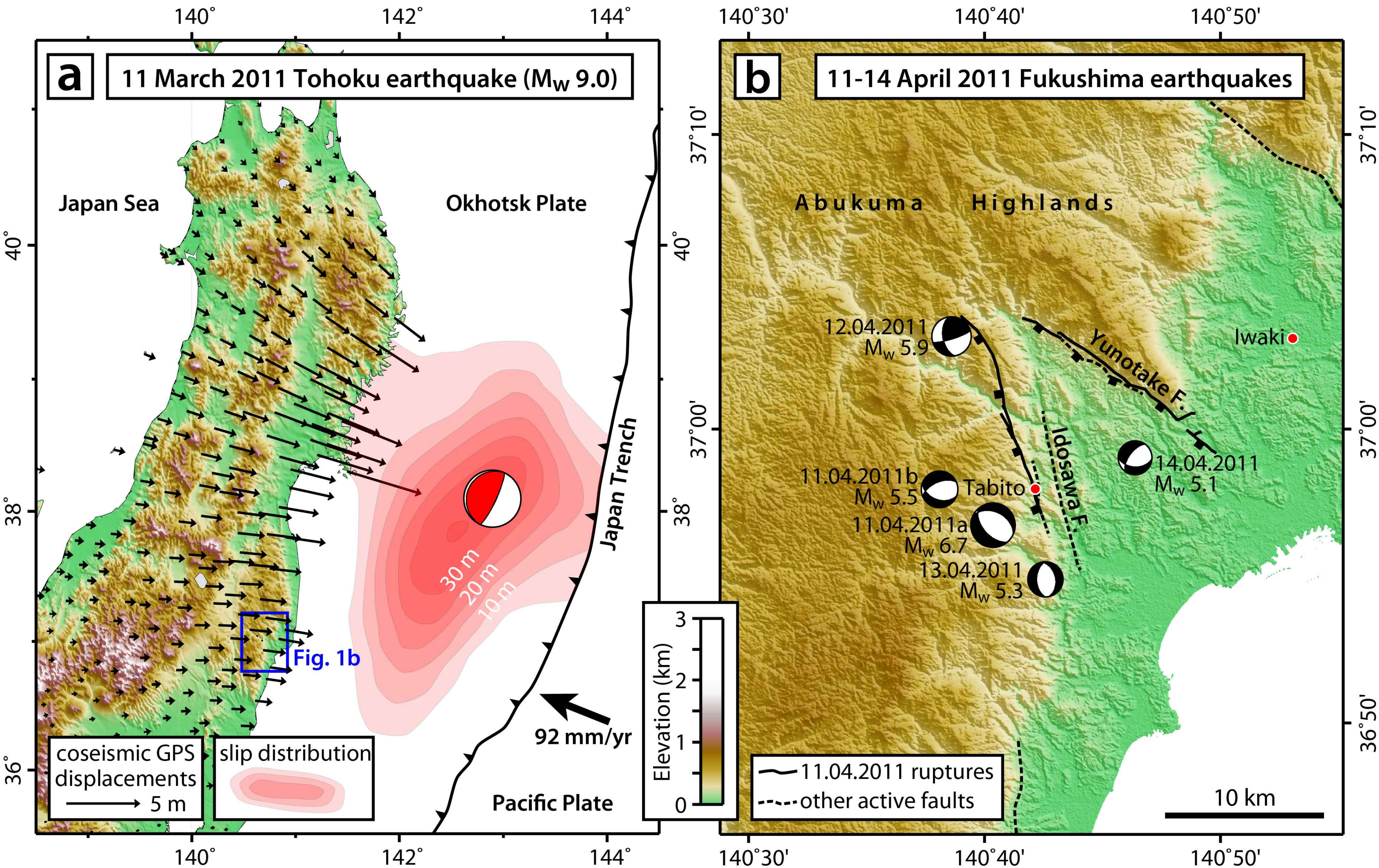

The 2011 Iwaki earthquake (Mw 6.7), Japan

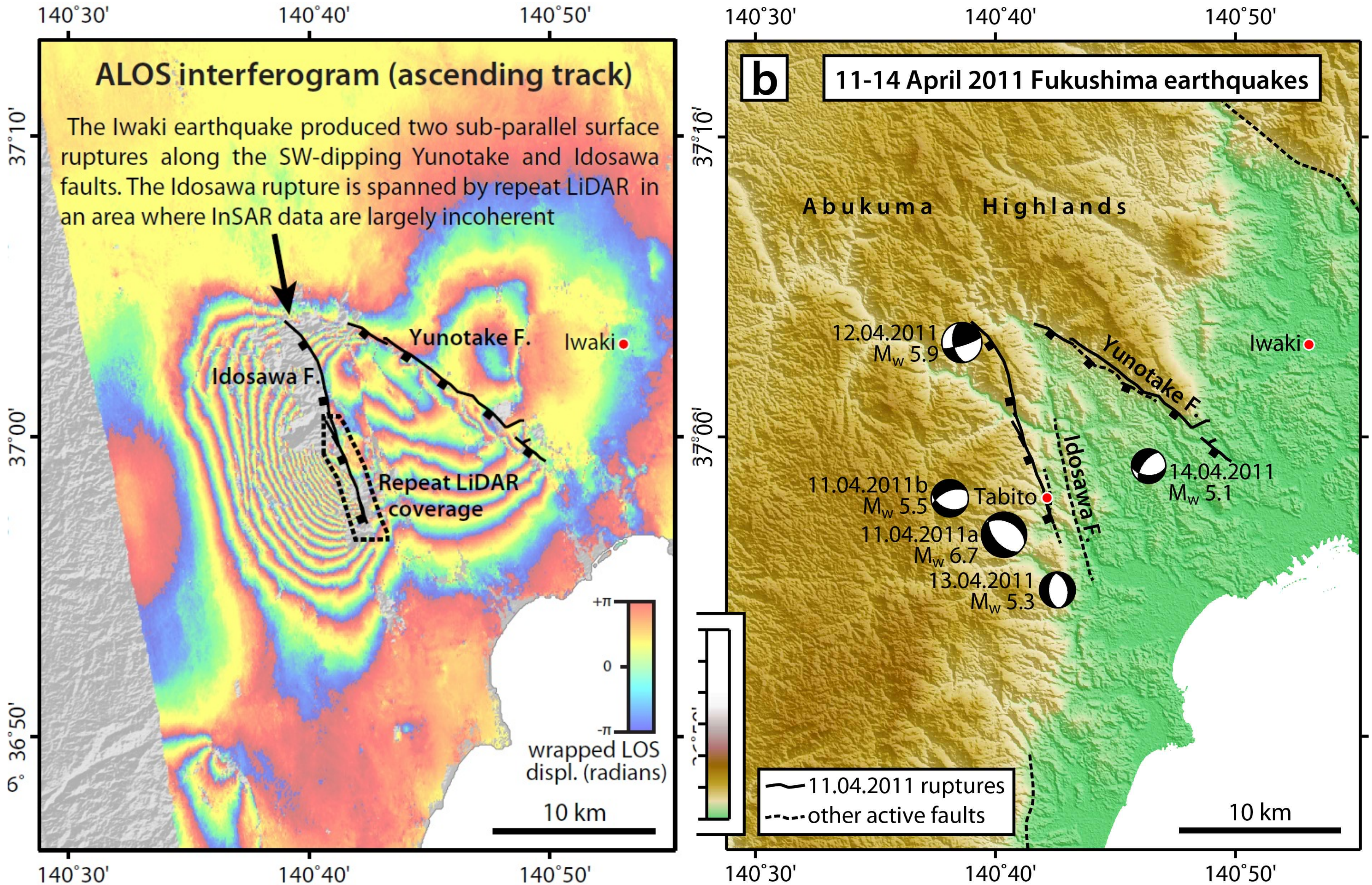

The 2011 Iwaki earthquake (Mw 6.7), Japan

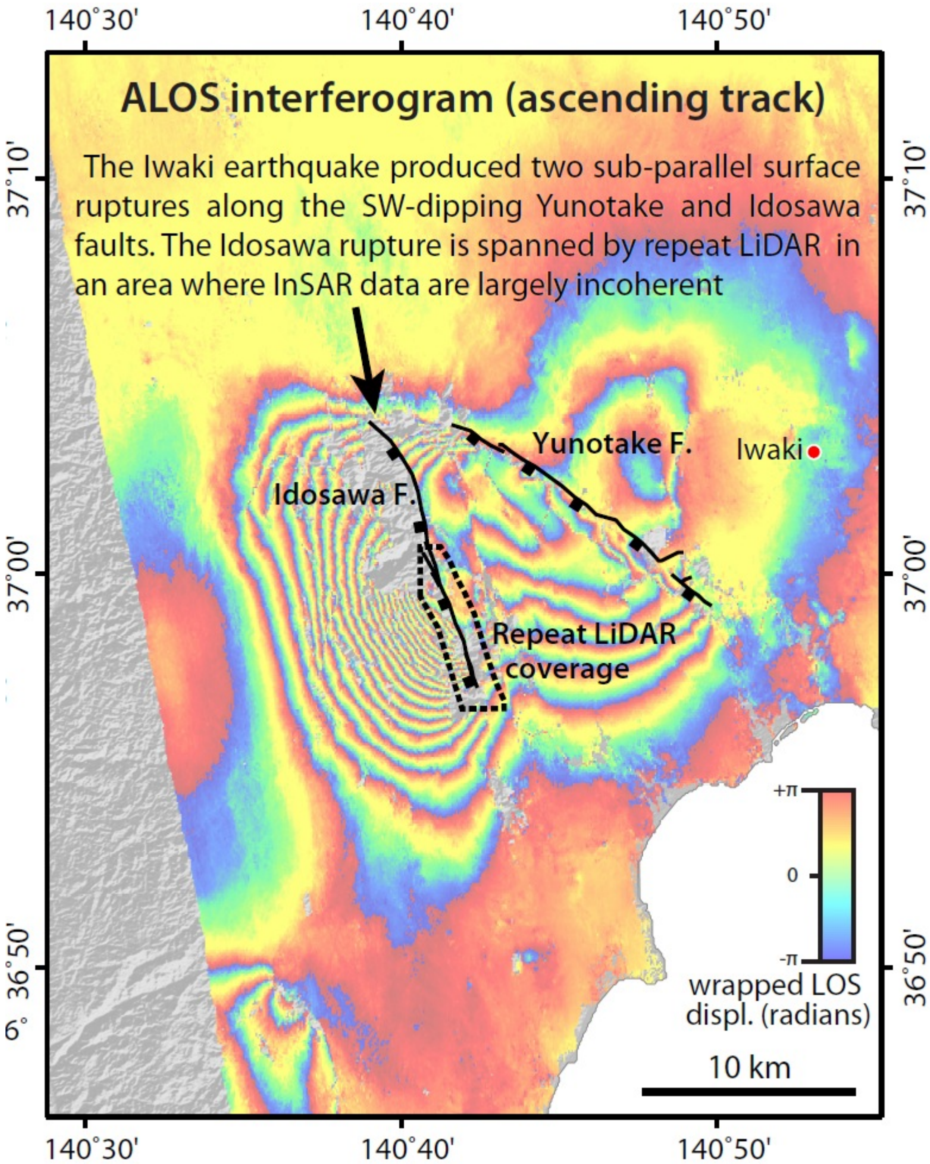

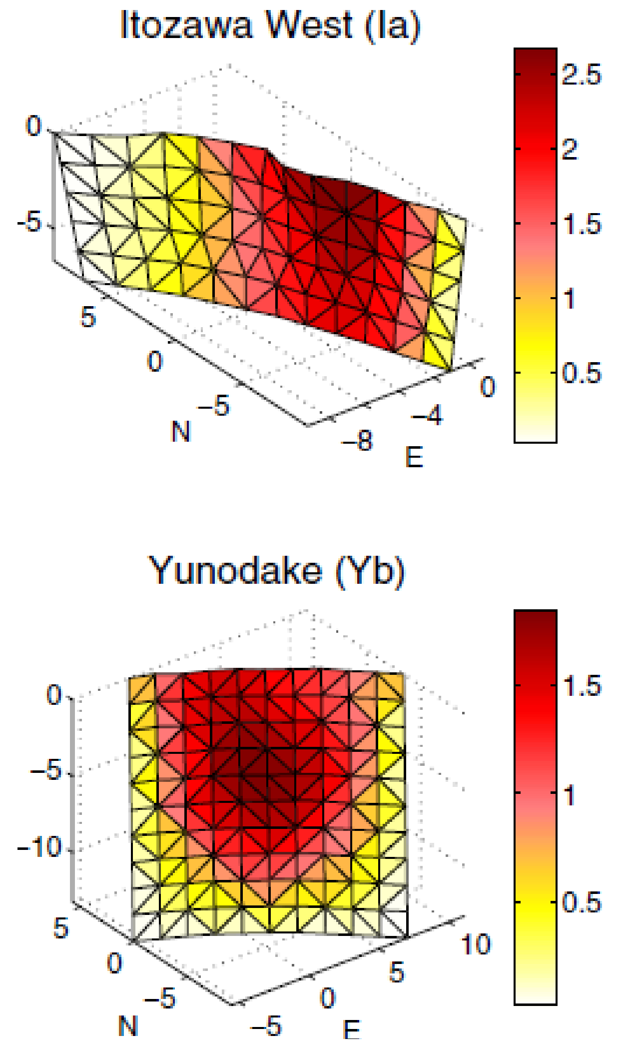

InSAR model from Fukushima et al. (2013), BSSA

The 2011 Iwaki earthquake (Mw 6.7), Japan

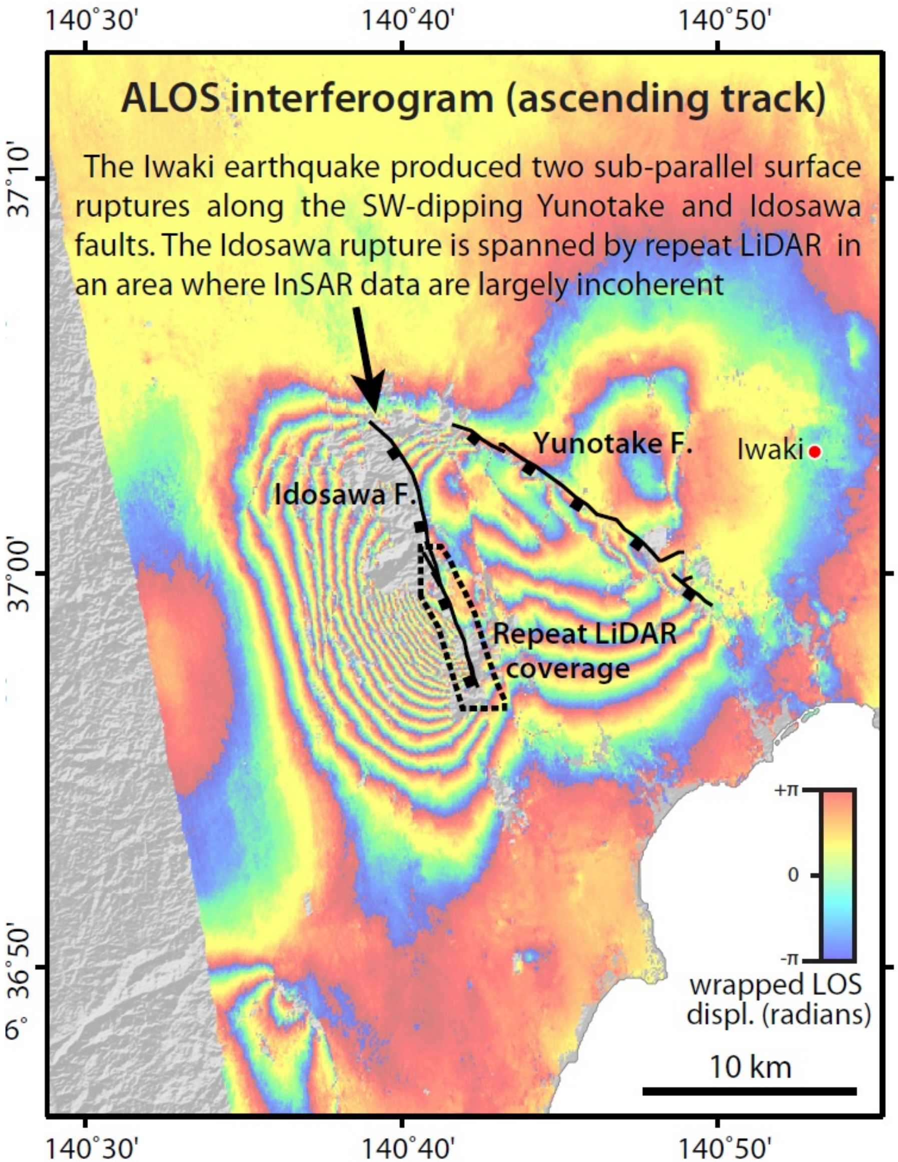

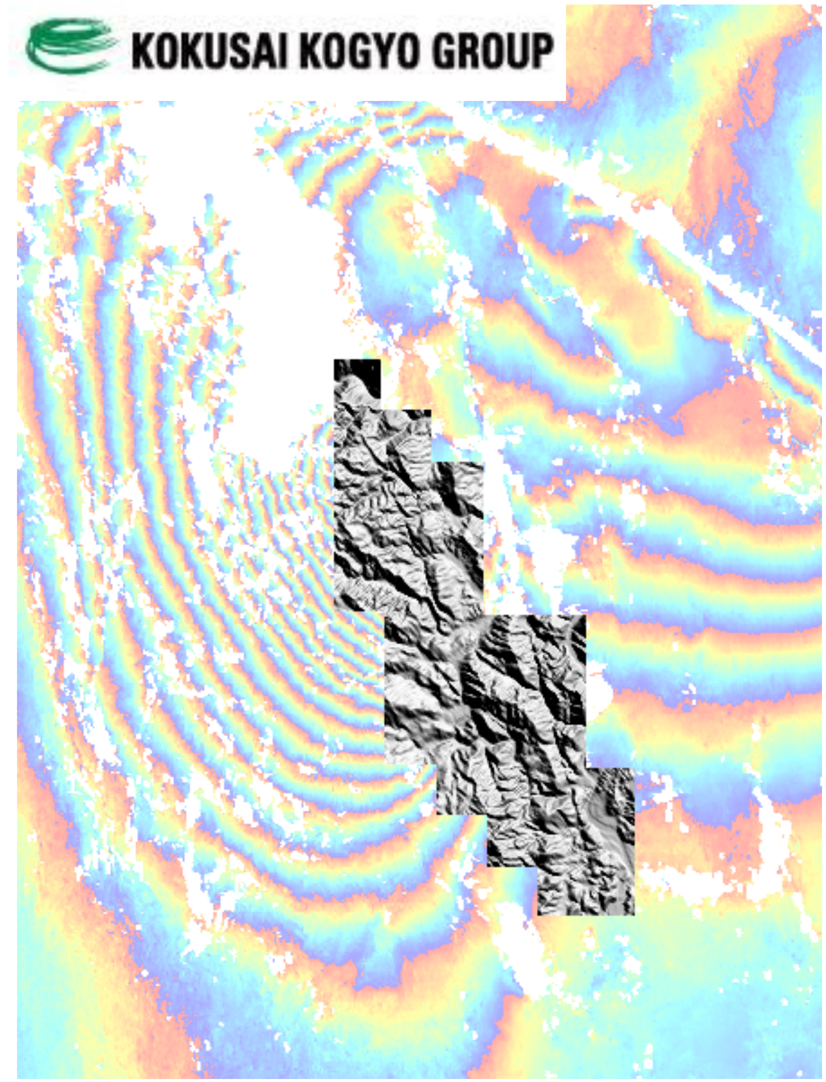

Pre-event data: 2 m Bare Earth DEM, Kokusai Kogyo Co. Ltd.

The 2011 Iwaki earthquake (Mw 6.7), Japan

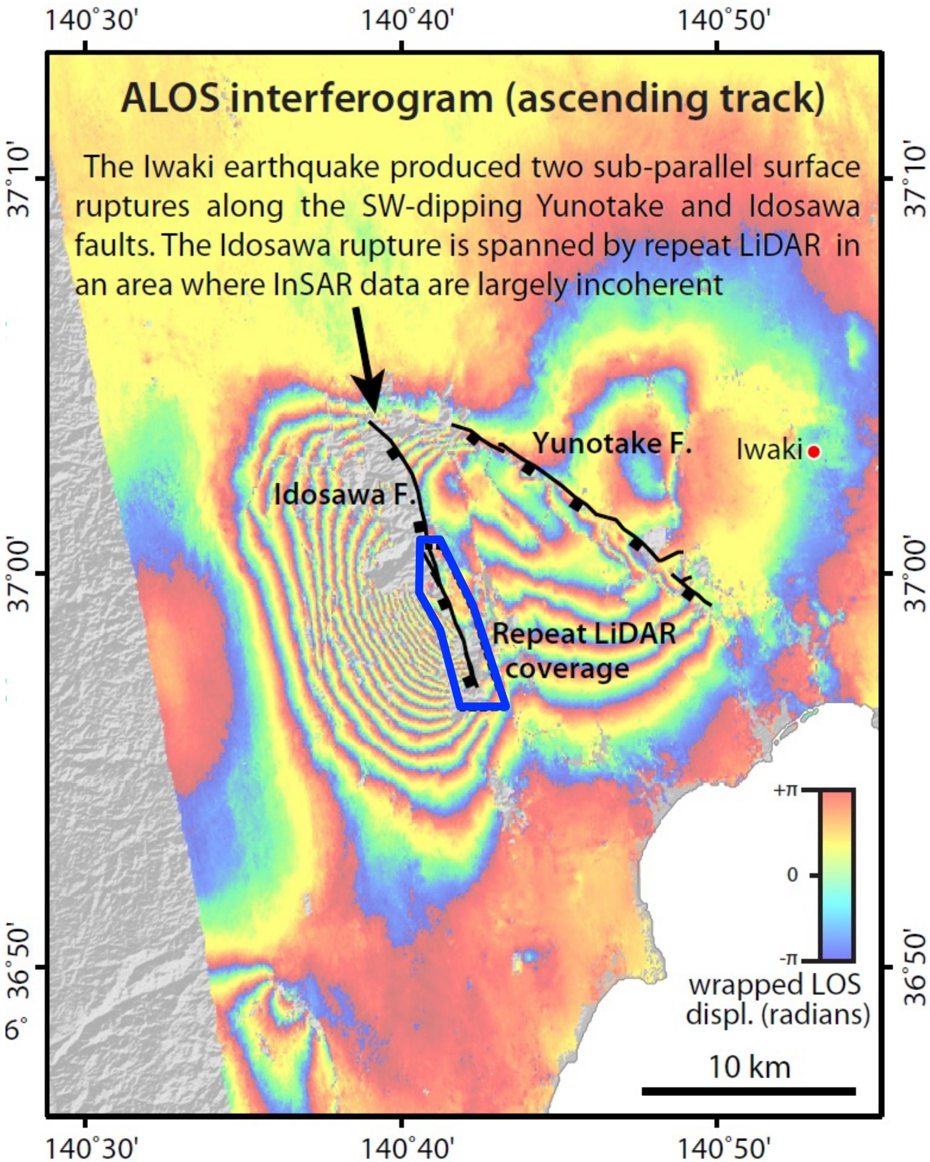

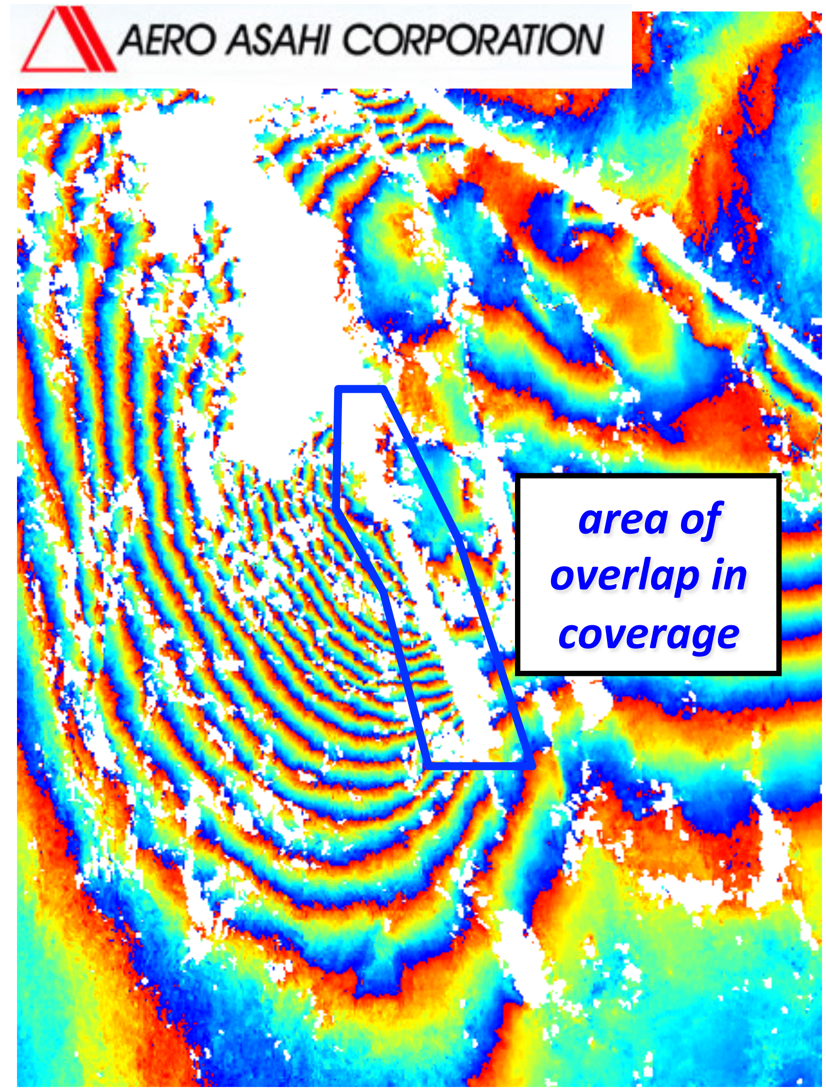

Post-event data: 1 m Bare Earth DEM, Aero Asahi Corp.

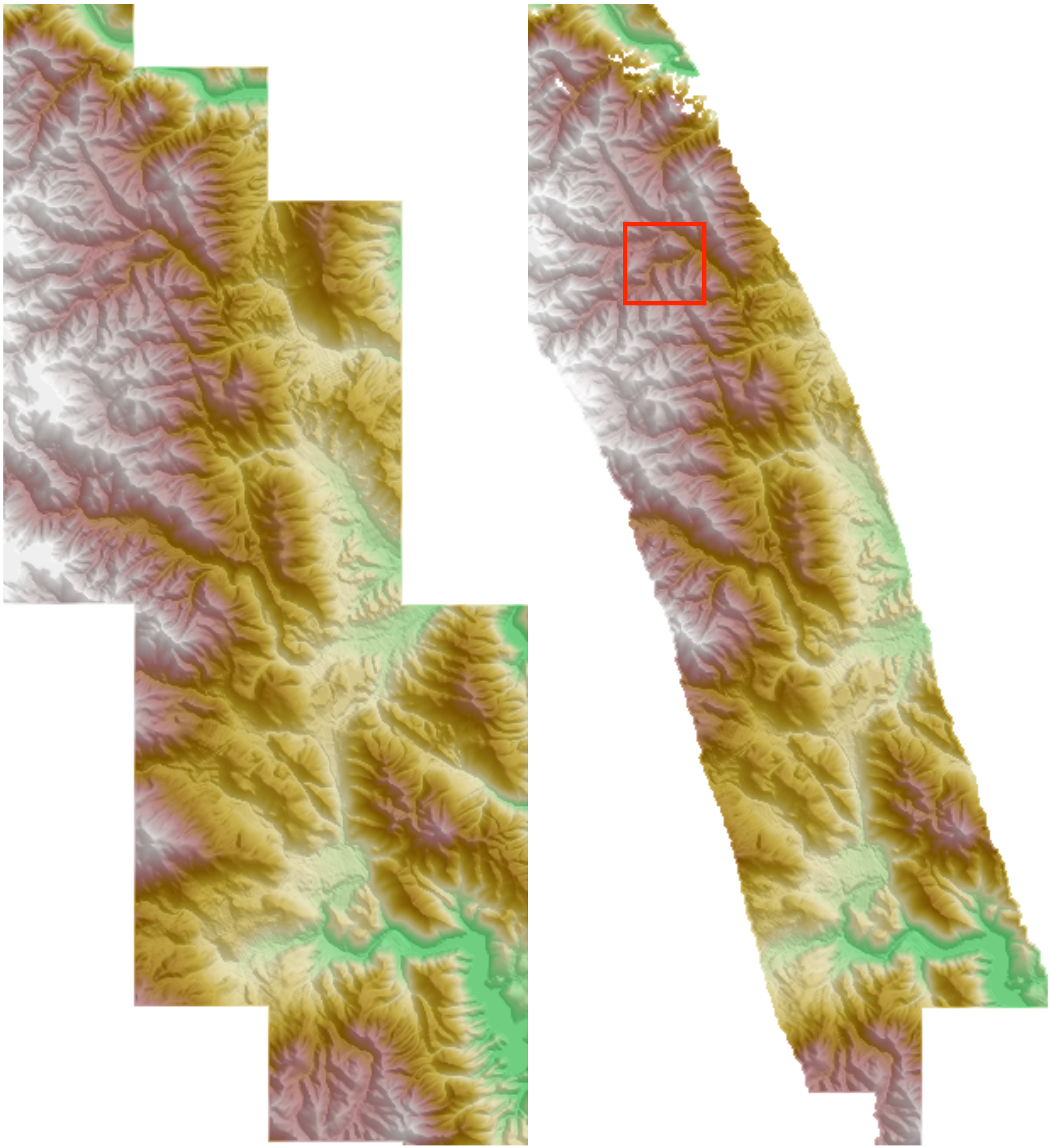

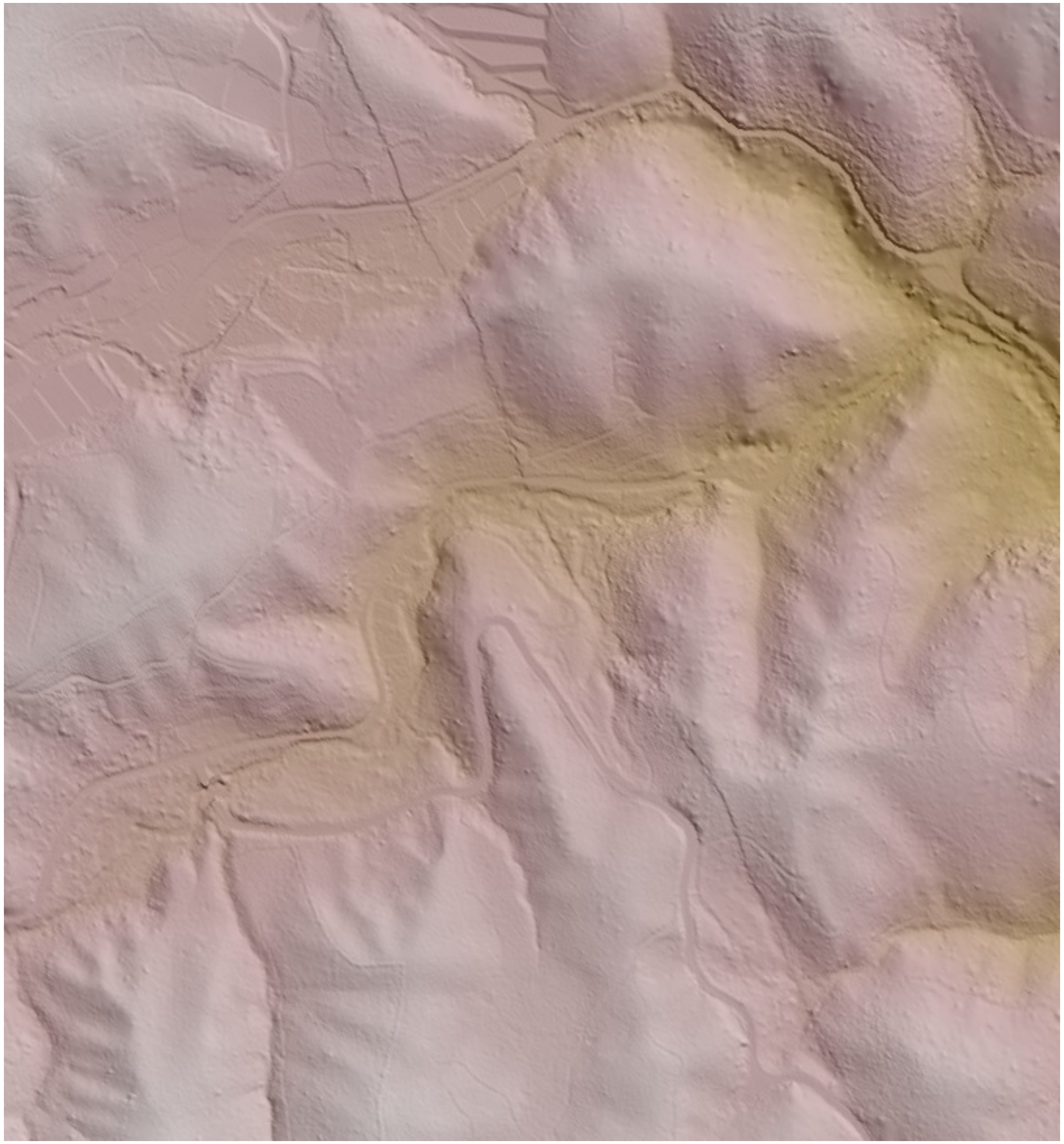

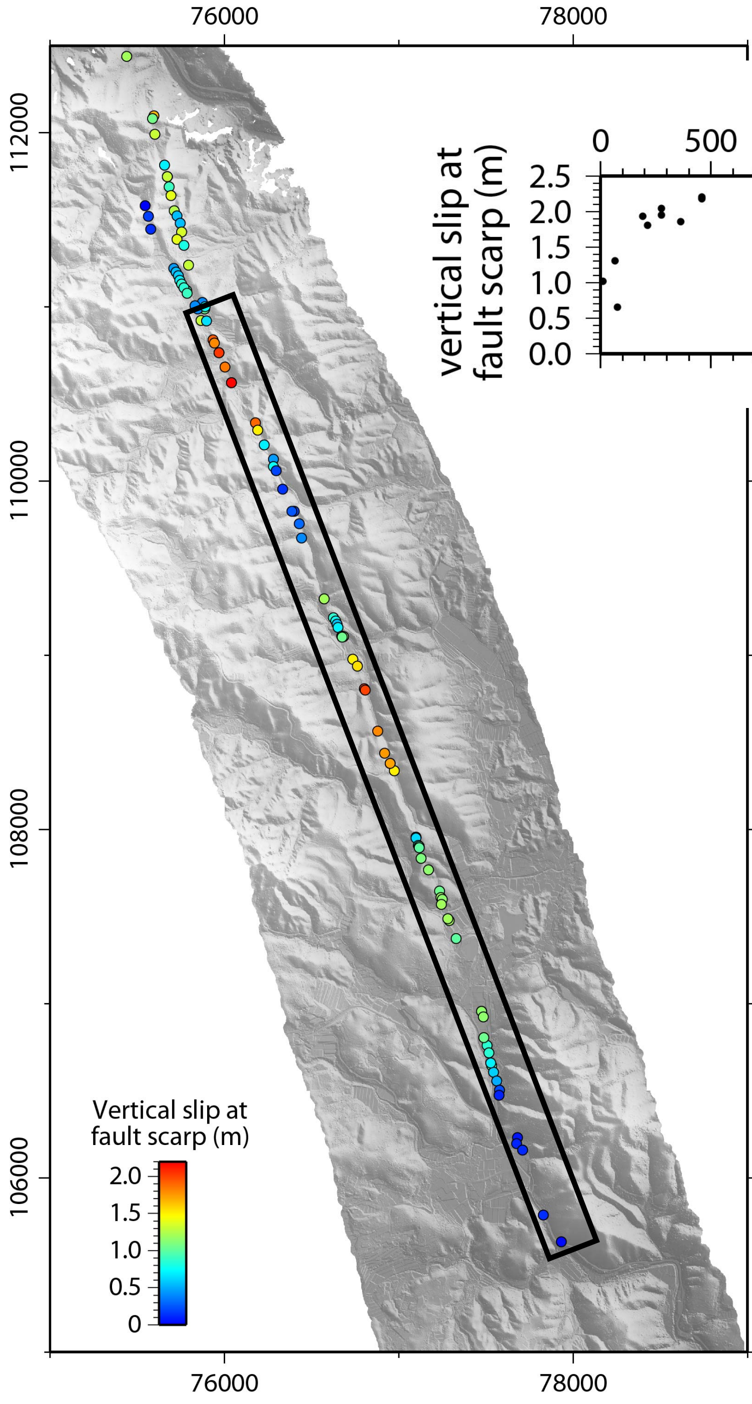

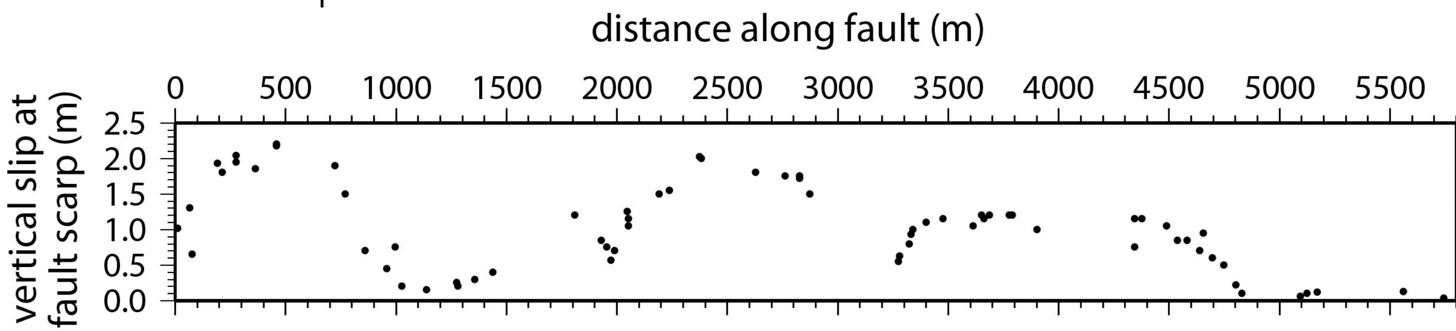

Field measurements of vertical fault slip by Tadashi Maruyama

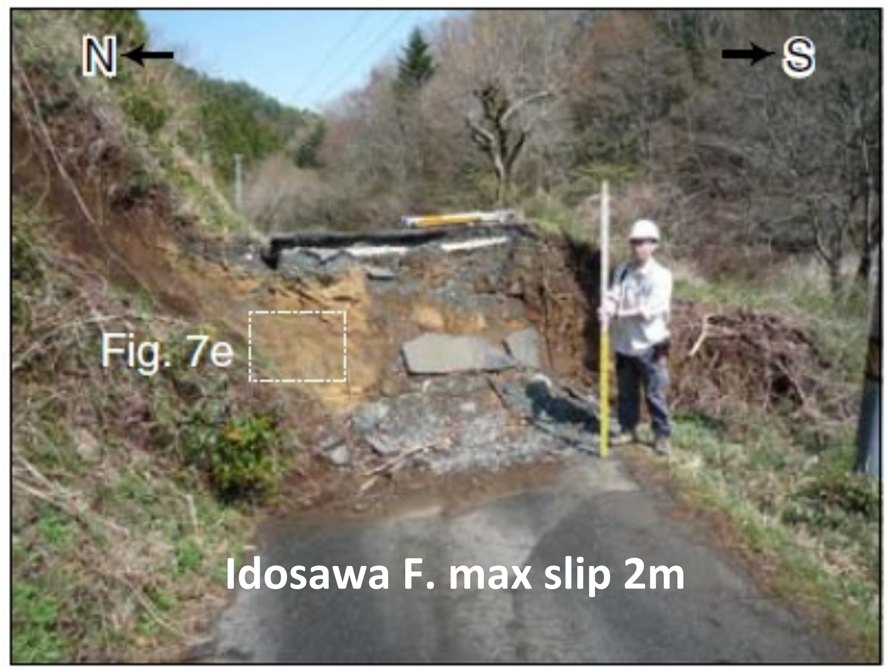

Toda & Tsutsumi (2013), Bull. Seism. Soc. Am.

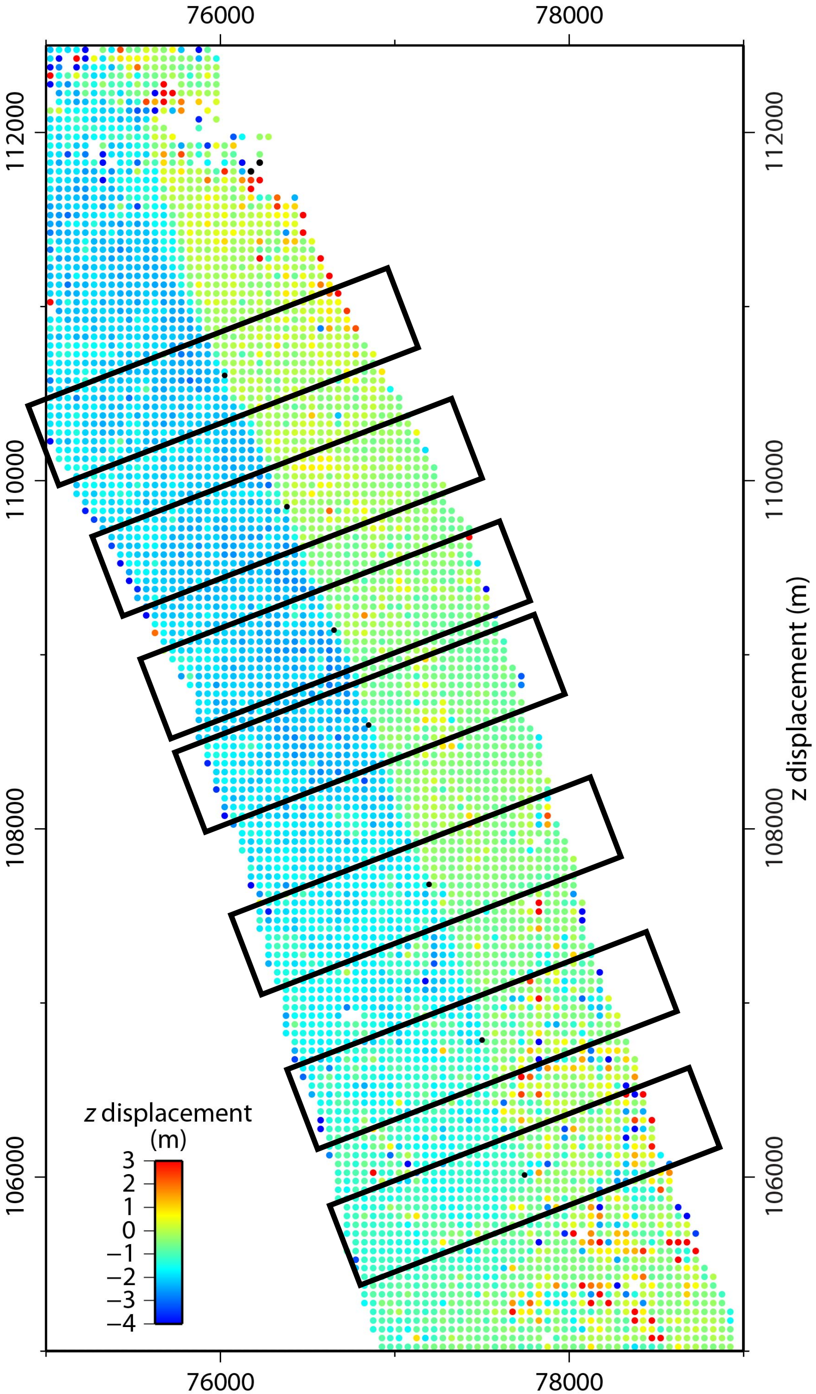

76000
78000
112000
110000
108000
106000
z displacement (m)
z displacement
(m)
3
2
1
0
−1
−2
−3
−4

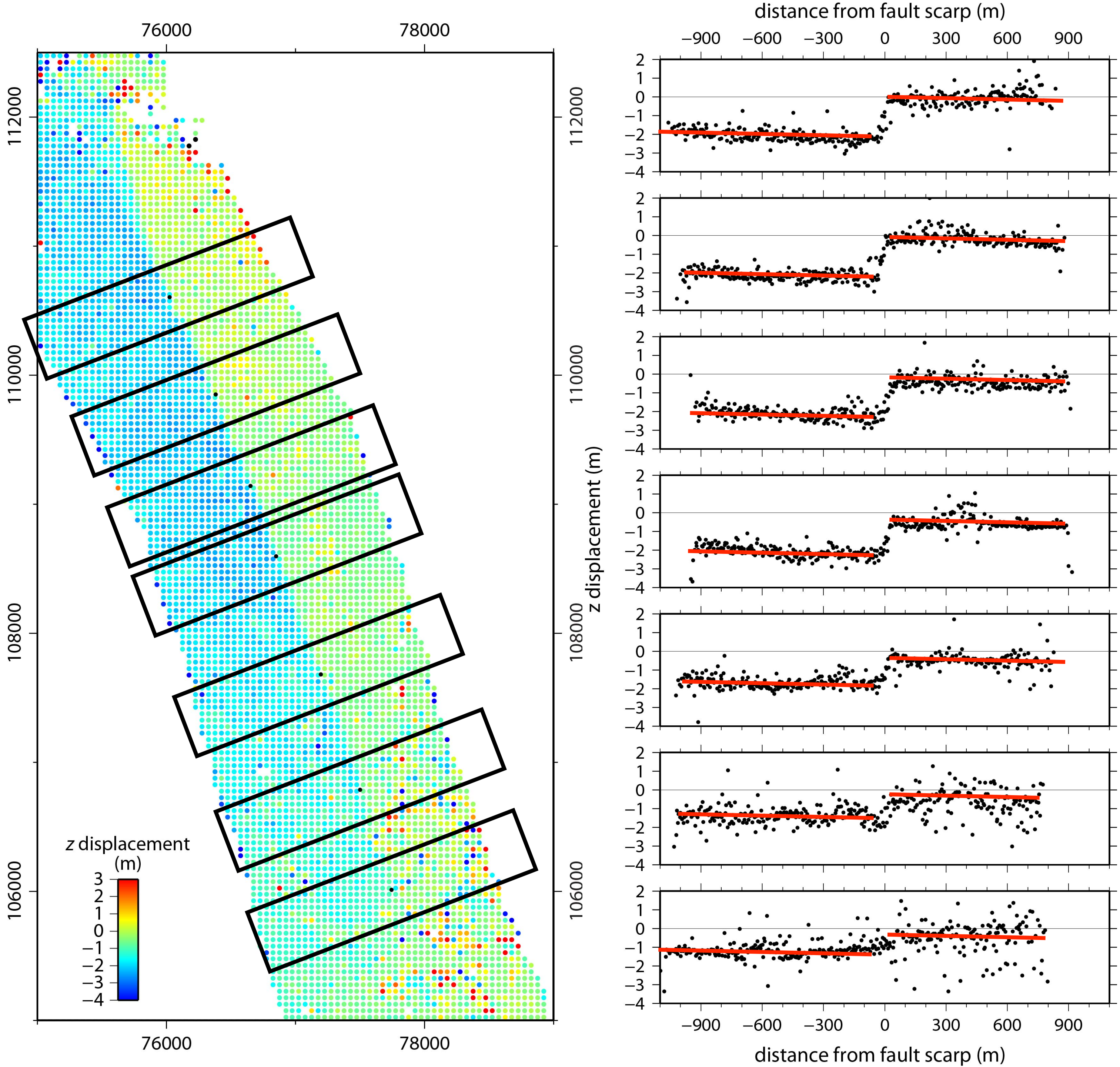

76000
78000
112000
110000
108000
106000
z displacement
(m)
3
2
1
0
−1
−2
−3
−4
distance from fault scarp (m)
−900
−600
−300
0
300
600
900
z displacement (m)

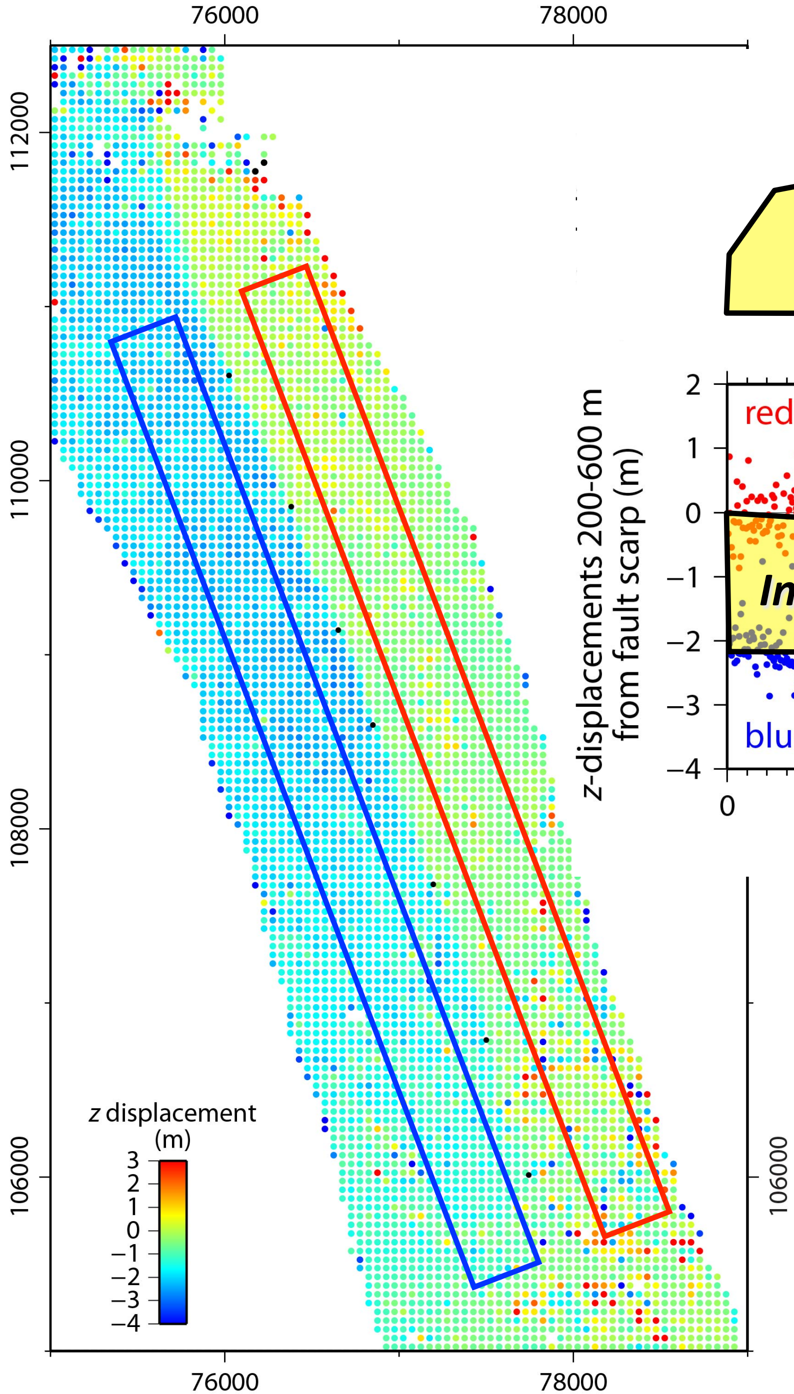

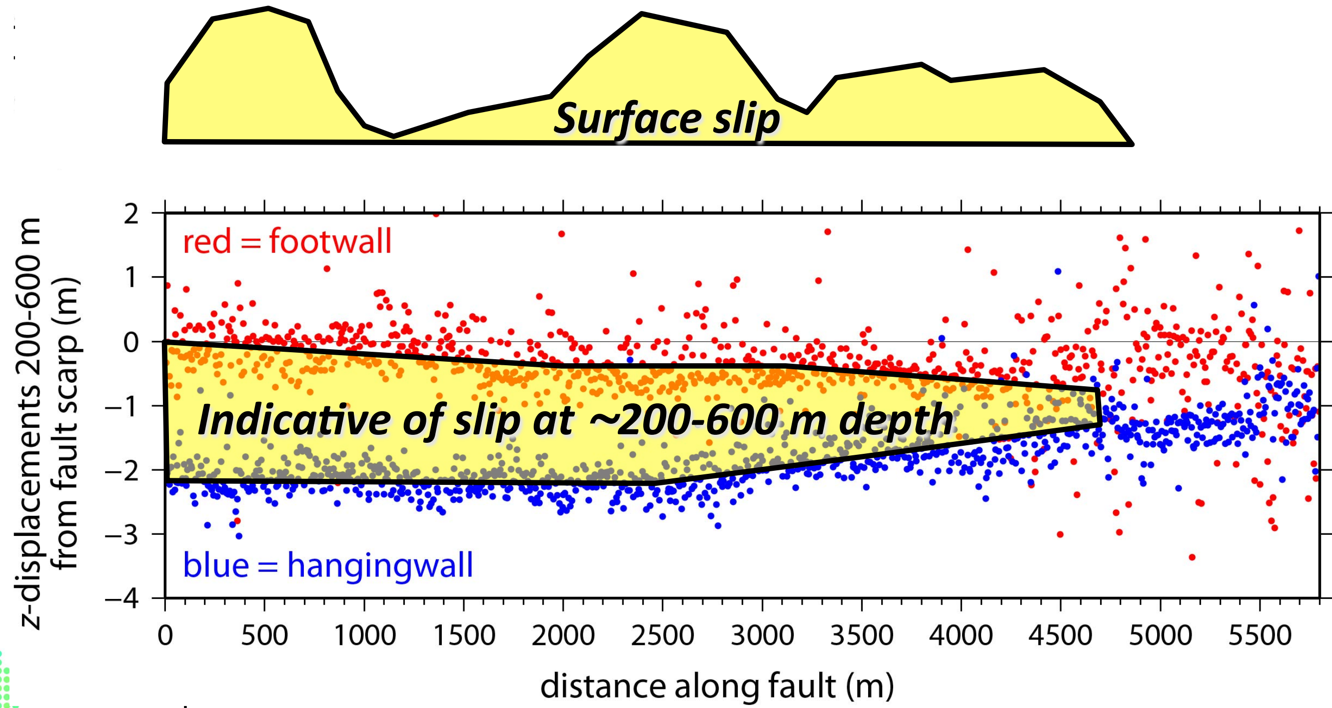

In many places, only a small proportion of the slip makes it to the surface

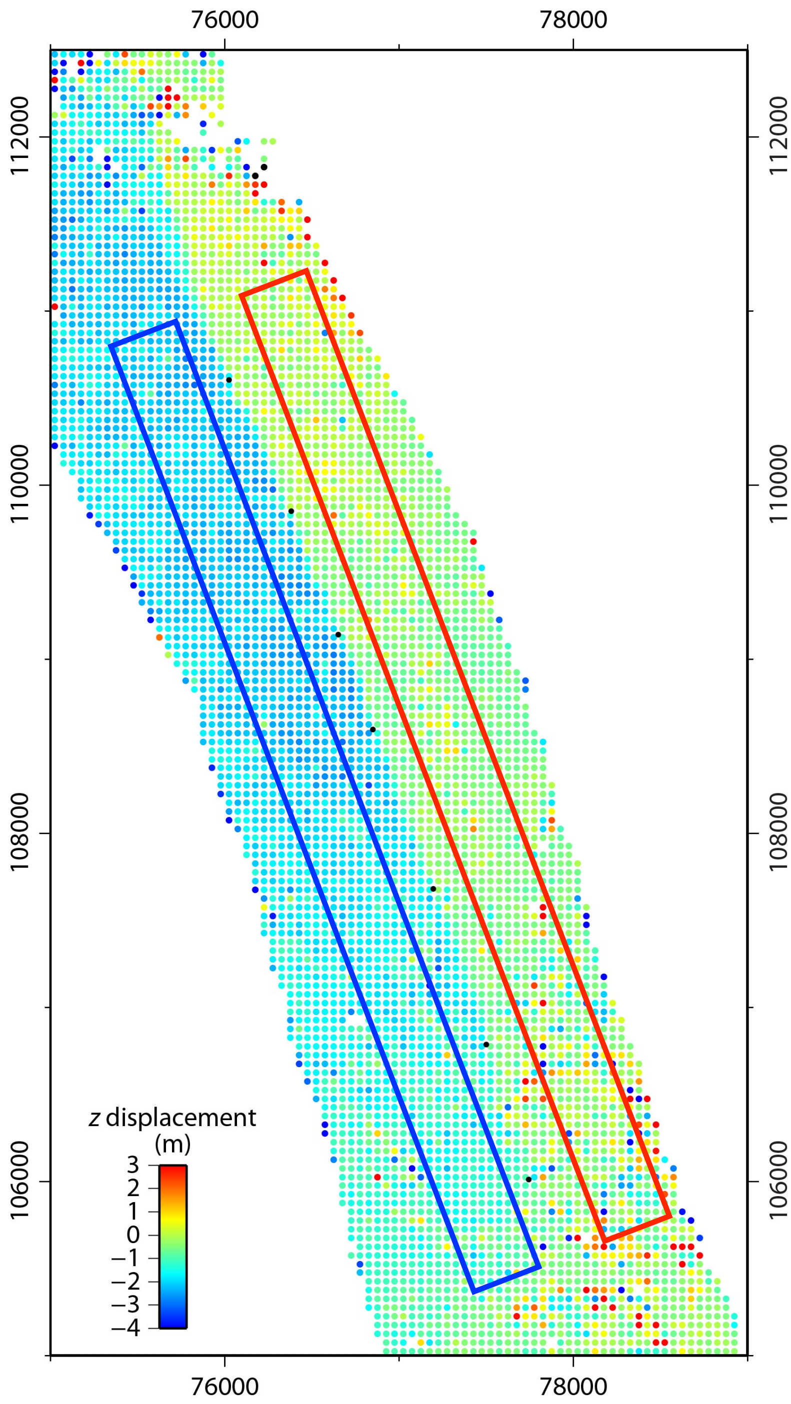

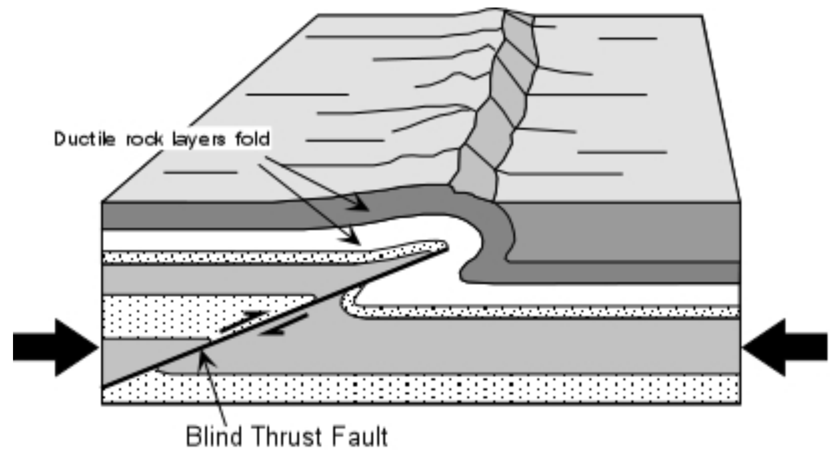

In many places, only a small proportion of the slip makes it to the surface

This is a common phenomenon for thrust faults that rupture upwards through unconsolidated sediment

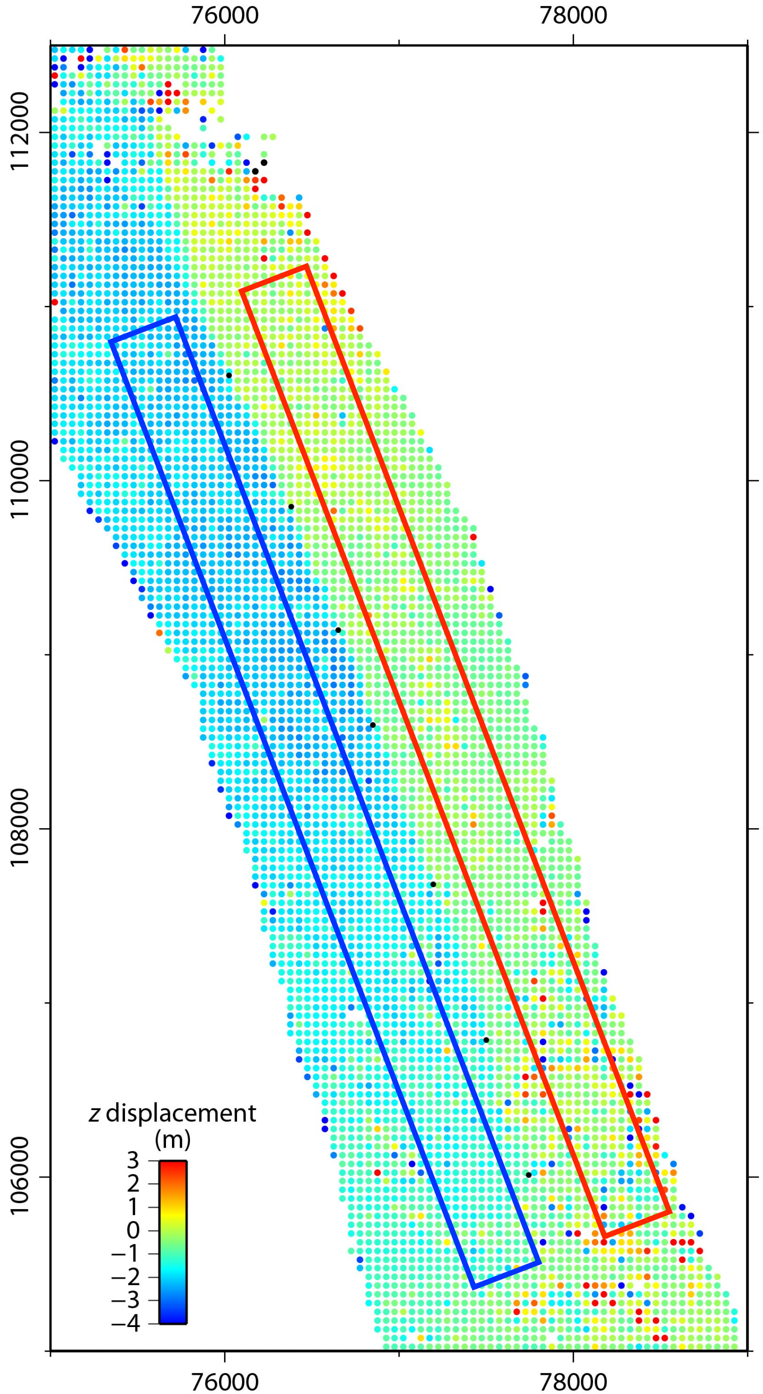

Geological map from Toda & Tsutsumi (2013)

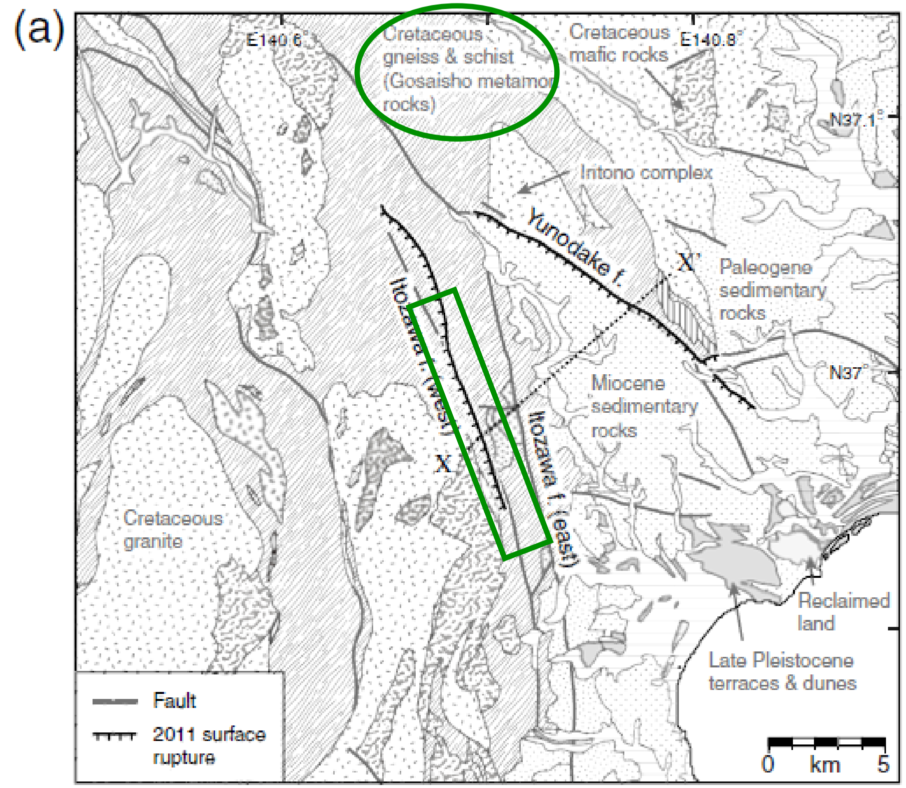

In many places, only a small proportion of the slip makes it to the surface

This is a common phenomenon for thrust faults that rupture upwards through unconsolidated sediment

However, this is a bedrock normal fault

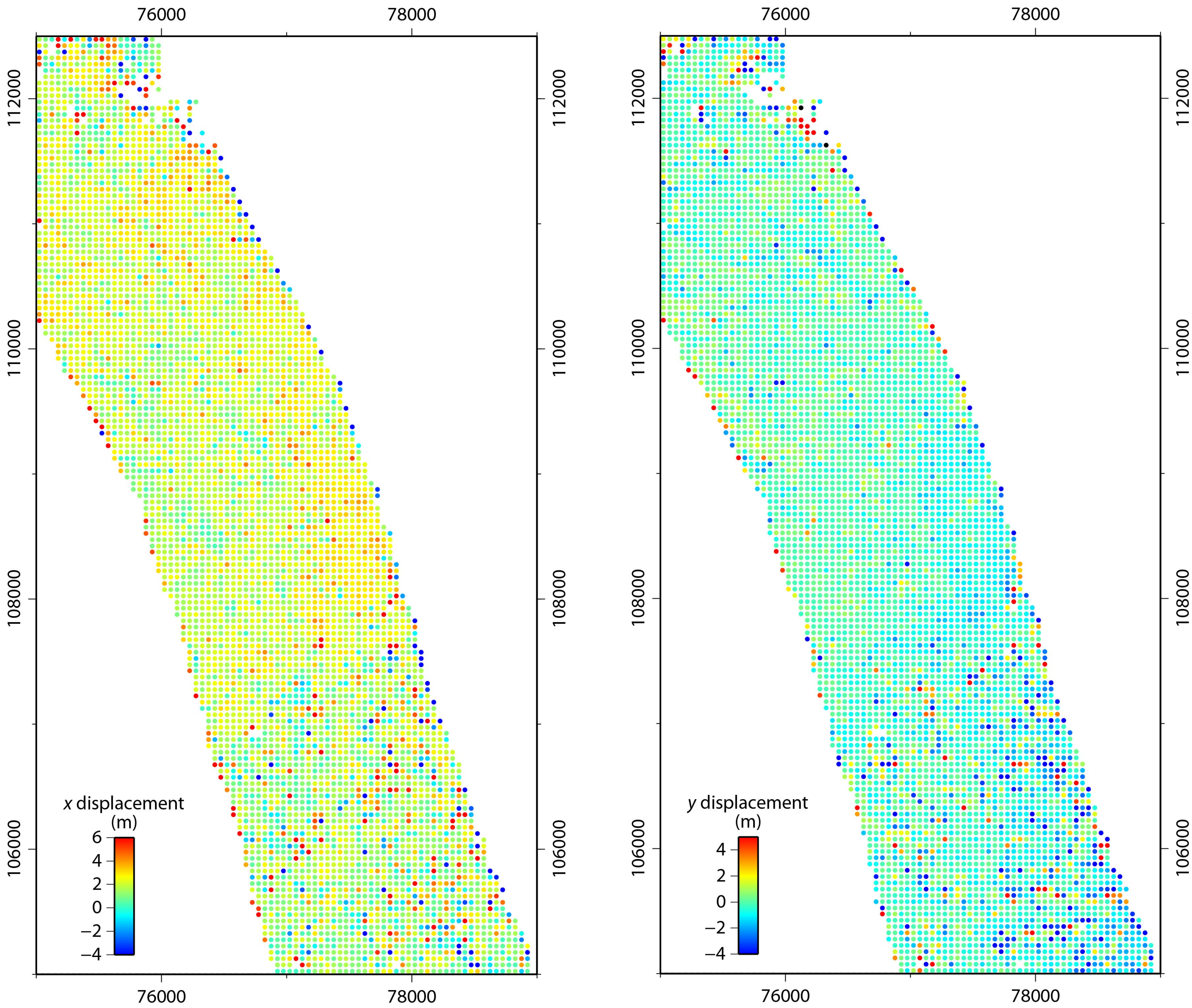
76000
78000
112000
110000
108000
106000
x displacement
(m)
6
4
2
0
−2
−4
y displacement
(m)
4
2
0
−2
−4

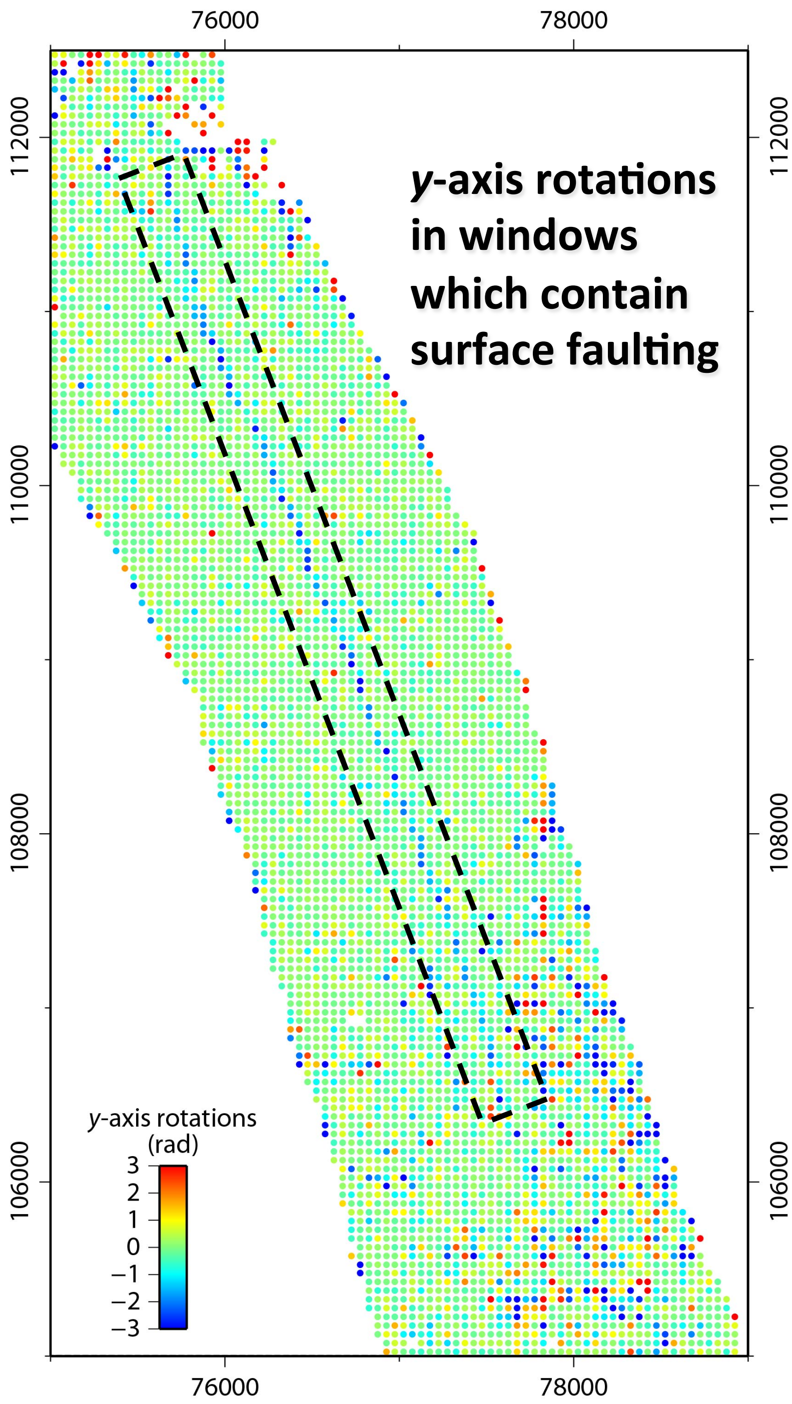
76000
78000
112000
110000
108000
106000
y-axis rotations
in windows
which contain
surface faulting
y-axis rotations
(rad)
3
2
1
0
−1
−2
−3

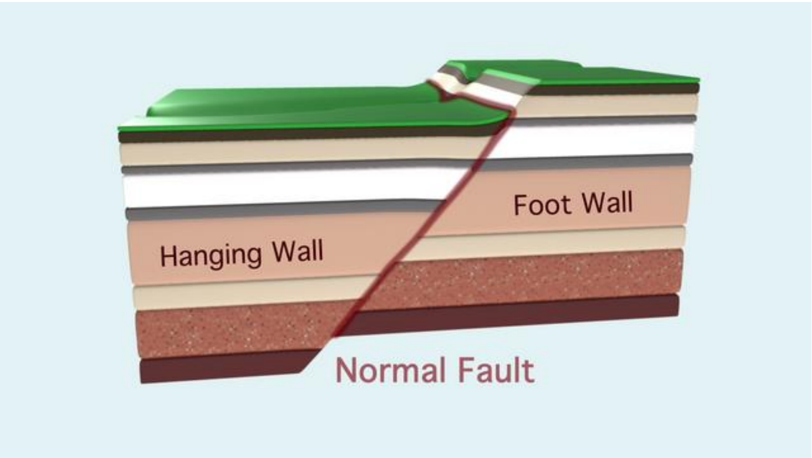
Foot Wall
Hanging Wall
Normal Fault

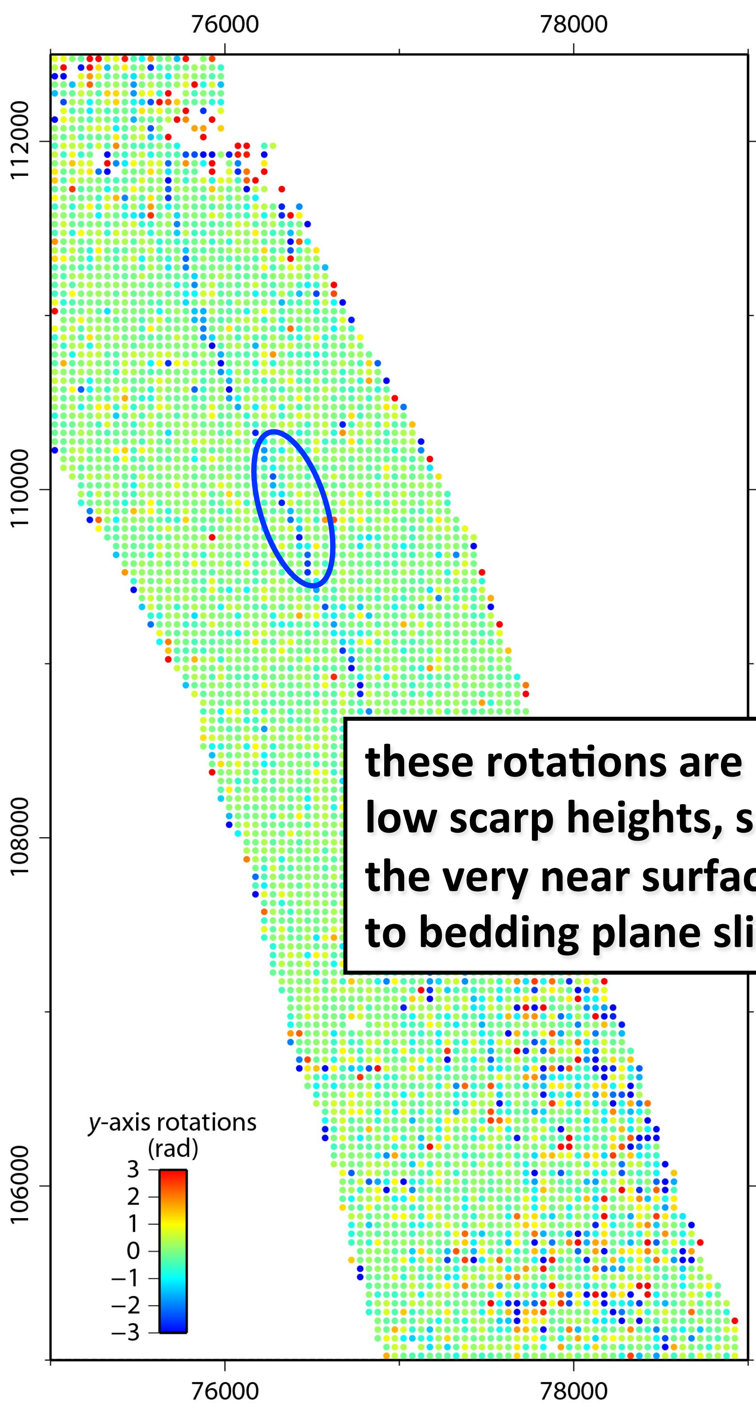

these rotations are present even in areas with low scarp heights, suggesting fault slip is lost in the very near surface (less than 50 m), perhaps to bedding plane slip or warping

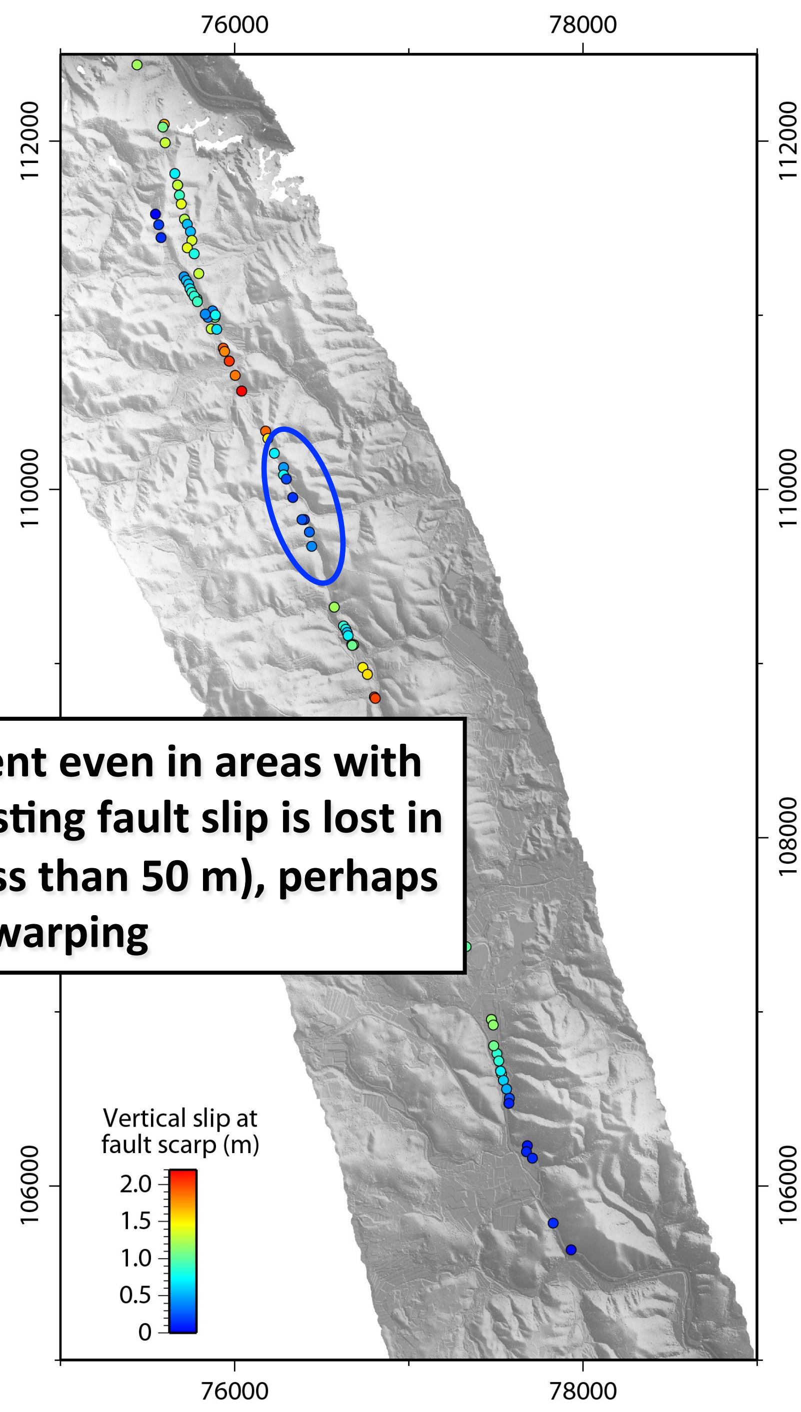

ICP LiDAR differencing: strengths and weaknesses

Synthetic Aperture Radar Interferometry (InSAR)

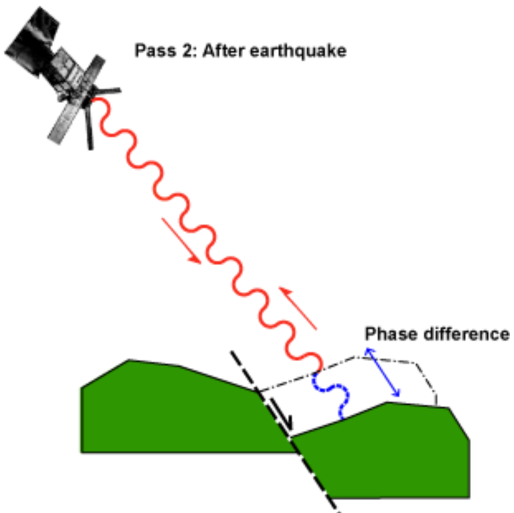

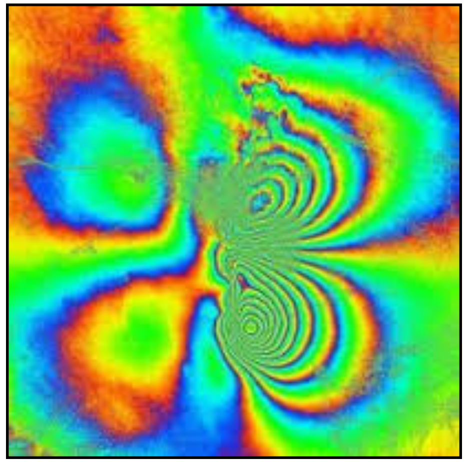

Sub-pixel matching

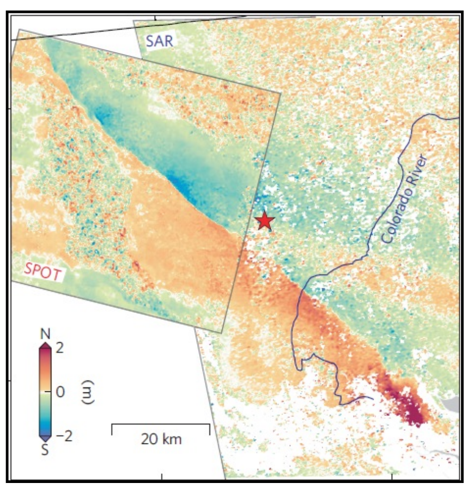

InSAR measures deformation in the satellite line of sight. **Pixel matching** usually only measures horizontal displacements.

*ICP can resolve displacements and rotations in **3-D.***

Pixel matching can be applied to LiDAR imagery, but requires gridding (rasterization) of the point clouds, resulting in information loss.

ICP works on the original point clouds.

InSAR is good at measuring **far-field deformation** but often break down close to surface faulting

*LiDAR is typically focused along active faults, so ICP will be useful for obtaining **near-field deformation***